UNIVERSITY OF CALIFORNIA SAN DIEGO

On the impact of neural variability on healthy aging and memory

A dissertation submitted in partial satisfaction
of the requirements for the degree Doctor of Philosophy

in

Neurosciences with a Specialization in Computational Neurosciences

by

Tam Thanh Tran

Committee in charge:

Professor Bradley Voytek, Chair
Professor Eric Halgren
Professor Marta Kutas
Professor Lara Rangel
Professor John Serences

2019

The Dissertation of Tam Thanh Tran is approved, and it is acceptable in quality and form for publication on microfilm and electronically:

_____

_____

_____

_____

_____

Chair

University of California San Diego

2019

DEDICATION

This dissertation is dedicated to Meghan, Mom, Dad, Tiffany, Timmy, Jupiter, Wolfie, and Mam, without whom this work would not have been possible.

TABLE OF CONTENTS

LIST OF FIGURES

ACKNOWLEDGEMENTS

I would like to acknowledge and thank first the members of the Voytek Lab for all of their help and support during my time at UCSD. Thank you, Brad, for taking me on as a student even though I had no background in electrophysiology or data analysis and for always being so supportive of my goals and interests both inside and outside the lab. Thank you, Richard, for always taking the time to explain things to me and for all of our conversations on academic research and our goals for the future. Thank you, Scott, for always pushing me to think about the next control analysis or another interpretation of my results. Thank you, Tom, for all of your Python and programming wisdom as well as all of the discussions we have had on brains, behavior, mentorship, and everything in between. Thank you, Roemer, for teaching me not only about ECoG and signal processing, but also about how the most important person to convince of anything is yourself. Thank you, Erik, for all you did in making lab fun and for guiding us graduate students through our early years in the lab.

I would also like to thank all members of the Book & Brunch Club. Our monthly meetings have been an absolute joy, something that has made these last years at UCSD not only easier, but also even more special.

Finally, I would like to acknowledge generous funding and support from the National Institute of Mental Health (NIMH) Training Program in Cognitive Neurosciences, the UCSD Institute for Neural Computation, the Kavli Institute for Brain and Mind, and the Achievement Rewards for College Scientists (ARCS) Foundation.

The introduction, in part, is an adaptation of the material as it appears in: Tran, T. T., Hoffner, N. C., LaHue, S. C., Tseng, L. & Voytek, B. Alpha phase dynamics predict

age-related visual working memory decline. NeuroImage 143, 196–203 (2016). Tran, T. T., Rolle, C. E., Gazzaley, A. & Voytek, B. Linked sources of neural noise contribute to age-related cognitive decline. Tran, T. T., Voytek, B. Frontal cortical aperiodic activity tracks successful memory encoding. The dissertation author was the primary investigator and author of these papers.

Chapter 1, in full, is a reprint of the material as it appears in: Tran, T. T., Hoffner, N. C., LaHue, S. C., Tseng, L. & Voytek, B. Alpha phase dynamics predict age-related visual working memory decline. NeuroImage 143, 196–203 (2016). The dissertation author was the primary investigator and author of this paper.

Chapter 2, in full, has been submitted for publication of the material. Tran, T. T., Rolle, C. E., Gazzaley, A. & Voytek, B. Linked sources of neural noise contribute to age-related cognitive decline. The dissertation author was the primary investigator and author of this paper.

Chapter 3, in full, is currently being prepared for submission for publication of the material. Tran, T. T. & Voytek B. Frontal cortical aperiodic activity tracks successful memory encoding. The dissertation author was the primary investigator and author of this paper.

VITA

2014 Bachelor of Science, University of California Los Angeles

2019 Doctor of Philosophy, University of California San Diego

2020 Scientific Analyst, Morrison & Foerster

PUBLICATIONS

Tran, T. T., Hoffner, N. C., LaHue, S. C., Tseng, L. & Voytek, B. Alpha phase dynamics predict age-related visual working memory decline. NeuroImage 143, 196–203 (2016).

Franklin, S., Kimball, T., Rasmussen, T., Rosa Garrido, M., Chen, H., Tran, T., Miller, M., Gray, R., Jiang, S., Ren, S., Wang, Y., Tucker, H & Vondriska, T. The chromatin binding protein Smyd1 restricts adult mammalian heart growth. American Journal of Physiology-Heart and Circulatory Physiology 311(5), 1234-1247 (2016).

ABSTRACT OF THE DISSERTATION

On the impact of neural variability on healthy aging and memory

by

Tam Thanh Tran

Doctor of Philosophy in Neurosciences with a Specialization in Computational Neurosciences

University of California San Diego, 2019

Professor Bradley Voytek, Chair

Herein I examine neural variability and its relationship to healthy aging and short-term memory. This variability is apparent not only in the inconsistency with which neural populations respond to and process incoming stimuli, but also in how ongoing neural activity fluctuates over time even in the absence of such stimuli. First, I show using electroencephalography (EEG) that higher trial-by-trial variability in the visual cortical alpha phase response to task-relevant stimuli is associated both with healthy aging and with reduced behavioral performance in a visual short-term memory task. Next, and also in EEG, I use the 1/*f*-like or aperiodic slope of the electrophysiological power spectrum to characterize baseline fluctuations in neural activity, and I show that in healthy aging, higher alpha phase response variability is associated with the age-related flattening of

the aperiodic slope of ongoing neural activity. Finally, I show using intracranial recordings that trial-by-trial shifts in the aperiodic slope of ongoing neural activity can help distinguish between episodes of successful versus unsuccessful memory encoding. I also show that shifts in ongoing neural activity index the number of items maintained and subsequently recalled from short-term memory. Altogether, these findings point to the continued need and utility of examining how neural variability, that in ongoing or in stimulus-evoked activity, can act as a neural signature both of age-related changes in behavior and of memory encoding and maintenance.

INTRODUCTION

Neural activity fluctuates over time even in the absence of external stimuli (Faisal et al., 2008). Such variability is seen at all measurement scales, from single-unit spiking to the fMRI BOLD signal. Though sometimes altogether referred to as “noise”, neural variability can nevertheless be separated into different components depending on task structure and demands (Dinstein et al., 2015). This separation allows for the exploration of various changes in neural activity uniquely associated with neuropsychiatric disorders, individual differences in behavior, and single-trial outcomes.

For instance, ongoing neural activity (that is, in the absence of or prior to the presentation of external stimuli) exhibits high trial-by-trial variability. This variability is significantly reduced or quenched upon stimulus presentation (Churchland et al., 2010; He, 2013), and the degree of quenching is predictive of individual differences in sensory processing and perception (Arazi et al., 2017). Trial-by-trial variability is also reduced by increases in alertness and attention (Mitchell et al., 2007; Arazi et al., 2019). These findings indicate that trial-by-trial neural variability has a direct effect on sensory processing and overall behavioral performance, as would be consistent with a signal detection framework in which gain and noise modulation both affect sensitivity. Additionally, increased trial-by-trial neural variability specifically in stimulus-evoked responses is linked to neurodevelopmental disorders including autism (Dinstein et al., 2012), dyslexia (Hornickel and Kraus, 2013), and attention deficit hyperactivity disorder (Saville et al., 2014). In the case of autism, such increases in the trial-by-trial variability of stimulus-evoked responses were not accompanied by high trial-by-trial variability in ongoing activity (Dinstein et al., 2012). This discrepancy further motivates the need to

explore different types of neural variability, their potentially dissociable sources, and their differential impacts on cognition and behavior.

Besides trial-by-trial neural variability, previous studies have also explored the amount or structure of fluctuations in ongoing neural activity on a single-trial basis. For example, the variance in ongoing neural activity has been examined and, for instance, shown to be increased in schizophrenia (Yang et al., 2014). Signal entropy measures have also been used to examine neural irregularity or signal complexity as they relate to perceptual performance (Waschke et al., 2017), memory formation (Sheehan et al., 2018), and aging (Waschke et al., 2017). Another method to examine such baseline variability in electrophysiological field potential recordings (or any other time series recording of neural activity) involves examining the shape of their corresponding power spectra. Neural activity is 1/*f*-like in that power deceases exponentially as a function of frequency (Pritchard, 1992; El Boustani et al., 2009; Miller et al., 2009; He et al., 2010; Gao, 2015). This 1/*f* component reflects the arrhythmic or aperiodic properties of neural activity and can be characterized using the linear slope and offset of log-log-space electrophysiological power spectra (He, 2014; Voytek et al., 2015; Haller et al., 2018). Any rhythmicity in neural activity, or neural oscillations, is indicated by the presence of peaks in the power spectra that exceed by some threshold the power of the 1/*f* component at neighboring frequencies (He, 2014; Voytek et al., 2015; Haller et al., 2018).

The 1/*f* slope of power spectra, or the rate of spectral power decrease as frequency increases, varies not only across individuals but also over time. For instance, 1/*f* slope is less negative or flatter in healthy older adults (Voytek et al., 2015; Waschke

et al., 2017; Dave et al., 2018) as well as in patients suffering from schizophrenia (Peterson et al., 2018), major depressive disorder (Veerakumar et al., 2019), or fibromyalgia (Gonzalez-Villar et al., 2017). Regarding 1/*f* slope and individual differences in cognitive performance, a recent study showed that individuals with flatter 1/*f* slope had higher performance on a verbal memory task (Sheehan et al, 2018). At the same time, 1/*f* slope within individuals varies between sleep and awake states (Freeman and Zhai, 2009; Veerakumar et al., 2019), flattens during visual stimulus presentation (Podvalny et al., 2015), and changes after the administration of anesthetic and other types of drugs (Gao et al., 2017; Muthukumaraswamy & Liley, 2018; Colombo et al., 2019). Some of these changes, particularly those drug-related, may track moment-to-moment fluctuations in excitatory-inhibitory (EI) ratio (Gao et al., 2017). Broadly, it has been hypothesized that a flattening of 1/*f* slope indexes the statistical structure of neural activity in that flatter slope might indicate weaker coupling between spiking activity and the local field potential (Voytek and Knight, 2015), possibly due to increases in EI ratio (Gao et al., 2017).

My goal is to extend this previous work by further exploring the relationships between various types of neural variability, healthy aging, and behavioral performance. In Chapter 1, I investigate age-related changes in the trial-by-trial variability of stimulus-evoked responses, examining in EEG how the visual cortical oscillatory alpha (7-14 Hz) phase response to a task-relevant alerting cue is altered in healthy aging. I find that trial-by-trial variability in the cue-evoked alpha phase response is heightened in older adults and that higher variability is related to reduced performance in younger adults during more demanding task conditions. Based on this finding, in Chapter 2 I explore

the relationship between baseline variability and trial-by-trial stimulus-evoked response variability in healthy aging. In examining baseline 1/*f* slope as well as the consistency of older adults' alpha phase response to visual targets in a visual discrimination task, I show that older adults with flatter visual cortical 1/*f* slope have the most inconsistent target-evoked alpha phase responses. This finding suggests that age-related changes in aperiodic activity, such changes apparent in the absence of external stimuli and potentially related to weaker spike-field coupling, might hamper older adults' ability to consistently respond to and process incoming stimuli.

I also extend previous work by exploring the relationship between baseline variability and single-trial behavioral performance. In electrocorticographic (ECoG) recordings from epileptic patients performing a delayed free recall task, I show that lateral frontal cortical 1/*f* slope is flatter prior to the presentation of subsequently recalled versus non-recalled words. I also find that lateral frontal cortical 1/*f* slope flattens over time as more items are maintained in memory. These findings suggest that a frontal cortical brain state in which spiking activity is only weakly coupled to the local field might improve the likelihood of successful memory encoding, subsequent recall, or both. These findings also suggest that such coupling further weakens in order to support the maintenance of more and more memory items. Altogether, Chapters 1 to 3 provide further evidence that changes in baseline aperiodic activity might impact sensory processing and cognitive performance, both broadly and in healthy aging. They also highlight the need for more research focused on how the changes in neural activity that lead to the flattening of 1/*f* slope might have differential impacts on behavior depending on task demands, subject demographics, or both.

Neural Variability in Healthy Aging

The neural noise hypothesis of aging proposes that healthy aging leads to diminished signal-to-noise in neural communication (Cremer and Zeef, 1987, Voytek & Knight, 2015). In support of this hypothesis, recent studies have shown age-related increases in EEG 1/*f*-like noise or slope and how these changes relate to alterations in cognitive performance (Voytek et al., 2015, Waschke et al., 2017; McNair et al., 2018). Potentially reflecting increased EI balance, these changes in baseline variability would be consistent with reported reduced inhibitory signaling in aging (Hickmott and Dinse, 2013).

In addition, the consistency of activity evoked by identical or near-identical stimuli, which is already highly variable across trials (Scholvinck et al., 2015), has also been found to be reduced in older adults. For instance, the amplitude and latency of various visual event-related potential (ERP) components can, depending on electrode locations and stimulus paradigms, be more variable in older adults (Kugler et al., 1993; Lorenzo-Lopez et al., 2007). Given concomitant age-related changes in baseline variability and increases in trial-by-trial, stimulus-evoked response variability, it is possible that alterations in baseline activity or variability might have a direct effect on the consistency with which older adults respond to and process external stimuli.

In this dissertation, we investigate the relationship between these two kinds of neural variability—tonic baseline variability and trial-by-trial, stimulus-evoked response variability—as well as their association with age-related cognitive decline. First, in Chapter 1, we explore in a combined visual attention and working memory task how age-related changes in alertness and spatial attention affect later working memory

performance. Specifically, we examine if age-related changes in neural activity manifest themselves in the magnitude and trial-by-trial consistency of the alpha amplitude and phase response to presentations of an alerting cue and a memory array.

Next, in Chapter 2, we use the 1/*f*-like power spectrum slope of pre-trial visual posterior neural activity to assess baseline variability during younger and older adults' performance of a visual discrimination task. To estimate trial-by-trial, stimulus-evoked response variability, we again measure the consistency of participants' oscillatory alpha phase response evoked by visual target presentation. We first replicate previous findings that older adults have altered baseline variability compared to and higher trial-by-trial response variability than younger adults, and we examine if older adults with greater changes in baseline variability – that is, significant increases in 1/*f* slope – also have higher trial-by-trial variability in stimulus-evoked responses.

Baseline Variability in Memory Encoding

In Chapter 3, we move to the examination of how baseline variability might affect behavioral performance on a single-trial basis, doing so in the context of memory formation. Successful memory encoding is associated with widespread changes in neural activity, for instance a decrease in power in lower frequencies and an increase in power in higher frequencies during the presentation of successfully versus unsuccessfully encoded memory items (Burke et al., 2013). Such differences have been observed in a number of brain regions, including the lateral temporal lobe (LTL) and the lateral frontal cortex (LFC), and have successfully been used to guide targeted electrical stimulation and rescue memory encoding (Ezzyat et al., 2018). However, it remains

unclear to what extent such observations are due to changes in oscillatory activity, aperiodic activity, or both. An increase or flattening of 1/*f* slope in response to visual stimulus presentation has previously been reported, such flattening synonymous with concomitant decreases and increases in lower- and higher-frequency activity, respectively (Podvalny et al., 2015). It is also not clear if such changes if present in baseline activity would also improve memory outcomes. In this dissertation, we investigate differences in baseline variability, specifically differences in 1/*f* slope, that predict successful versus unsuccessful memory encoding. We also examine if changes in 1/*f* slope over time contain information about the number of items maintained in memory.

The introduction, in part, is an adaptation of the material as it appears in: Tran, T. T., Hoffner, N. C., LaHue, S. C., Tseng, L. & Voytek, B. Alpha phase dynamics predict age-related visual working memory decline. NeuroImage 143, 196–203 (2016). The dissertation author was the primary investigator and author of this paper.

The introduction, in part, is an adaptation of material that has been submitted for publication. Tran, T. T., Rolle, C. E., Gazzaley, A. & Voytek, B. Linked sources of neural noise contribute to age-related cognitive decline. The dissertation author was the primary investigator and author of these papers.

The introduction, in part, is an adaptation of material currently being prepared for submission for publication. Tran, T. T., Voytek, B. Frontal cortical aperiodic activity tracks successful memory encoding. The dissertation author was the primary investigator and author of these papers.

References

Arazi, A., Censor, N., Dinstein, I., 2017. Neural Variability Quenching Predicts Individual Perceptual Abilities. J. Neurosci. 37, 97–109.

Arazi, A., Yeshurun, Y., Dinstein, I., 2019. Neural Variability Is Quenched by Attention. J. Neurosci. 39, 5975–5985.

Boustani, El, S., Marre, O., Béhuret, S., Baudot, P., Yger, P., Bal, T., Destexhe, A., Frégnac, Y., 2009. Network-state modulation of power-law frequency-scaling in visual cortical neurons. PLoS Comput Biol 5, e1000519.

Burke, J.F., Zaghloul, K.A., Jacobs, J., Williams, R.B., Sperling, M.R., Sharan, A.D., Kahana, M.J., 2013. Synchronous and asynchronous theta and gamma activity during episodic memory formation. J. Neurosci. 33, 292–304.

Churchland, M.M., Yu, B.M., Cunningham, J.P., Sugrue, L.P., Cohen, M.R., Corrado, G.S., Newsome, W.T., Clark, A.M., Hosseini, P., Scott, B.B., Bradley, D.C., Smith, M.A., Kohn, A., Movshon, J.A., Armstrong, K.M., Moore, T., Chang, S.W., Snyder, L.H., Lisberger, S.G., Priebe, N.J., Finn, I.M., Ferster, D., Ryu, S.I., Santhanam, G., Sahani, M., Shenoy, K.V., 2010. Stimulus onset quenches neural variability: a widespread cortical phenomenon. Nature Neuroscience 13, 369–378.

Colombo, M.A., Napolitani, M., Boly, M., Gosseries, O., Casarotto, S., Rosanova, M., Brichant, J.-F., Boveroux, P., Rex, S., Laureys, S., Massimini, M., Chieregato, A., Sarasso, S., 2019. The spectral exponent of the resting EEG indexes the presence of consciousness during unresponsiveness induced by propofol, xenon, and ketamine. NeuroImage 189, 631–644.

Cremer, R., Zeef, E.J., 1987. What Kind of Noise Increases With Age? Journal of Gerontology 42, 515–518.

Dave, S., Brothers, T.A., Swaab, T.Y., 2018. 1/ f neural noise and electrophysiological indices of contextual prediction in aging. Brain Research 1691, 34–43.

Dinstein, I., Heeger, D.J., Behrmann, M., 2015. Neural variability: friend or foe? Trends in Cognitive Sciences 19, 322–328.

Dinstein, I., Heeger, D.J., Lorenzi, L., Minshew, N.J., Malach, R., Behrmann, M., 2012. Unreliable Evoked Responses in Autism. Neuron 75, 981–991.

Ezzyat, Y., Wanda, P.A., Levy, D.F., Kadel, A., Aka, A., Pedisich, I., Sperling, M.R., Sharan, A.D., Lega, B.C., Burks, A., Gross, R.E., Inman, C.S., Jobst, B.C., Gorenstein, M.A., Davis, K.A., Worrell, G.A., Kucewicz, M.T., Stein, J.M., Gorniak, R., Das, S.R., Rizzuto, D.S., Kahana, M.J., 2018. Closed-loop stimulation of

temporal cortex rescues functional networks and improves memory. Nat Comms 9, 365–8.

Faisal, A.A., Selen, L.P.J., Wolpert, D.M., 2008. Noise in the nervous system. Nat Rev Neurosci 9, 292–303.

Freeman, W.J., Zhai, J., 2009. Simulated power spectral density (PSD) of background electrocorticogram (ECoG). Cogn Neurodyn 3, 97–103.

Gao, R., 2016. Interpreting the electrophysiological power spectrum. Journal of Neurophysiology 115, 628–630.

Gao, R., Peterson, E.J., Voytek, B., 2017. Inferring synaptic excitation/inhibition balance from field potentials. NeuroImage 158, 70–78.

González-Villar, A.J., Samartin-Veiga, N., Arias, M., Carrillo-de-la-Peña, M.T., 2017. Increased neural noise and impaired brain synchronization in fibromyalgia patients during cognitive interference. Scientific Reports 7, 5841–8.

Haller, M., Donoghue, T., Peterson, E., Varma, P., Sebastian, P., Gao, R., Noto, T., Knight, R.T., Shestyuk, A., Voytek, B., 2018. Parameterizing neural power spectra. bioRxiv 299859.

He, B.J., 2013. Spontaneous and Task-Evoked Brain Activity Negatively Interact. Journal of Neuroscience 33, 4672–4682.

He, B.J., 2014. Scale-free brain activity: past, present, and future. Trends in Cognitive Sciences 18, 480–487.

He, B.J., Zempel, J.M., Snyder, A.Z., Raichle, M.E., 2010. The Temporal Structures and Functional Significance of Scale-free Brain Activity. Neuron 66, 353–369.

Hickmott, P., Dinse, H., 2013. Effects of Aging on Properties of the Local Circuit in Rat Primary Somatosensory Cortex (S1) In Vitro. Cerebral Cortex 23, 2500–2513.

Hornickel, J., Kraus, N., 2013. Unstable Representation of Sound: A Biological Marker of Dyslexia. Journal of Neuroscience 33, 3500–3504.

Kügler, C.F., Taghavy, A., Platt, D., 1993. The event-related P300 potential analysis of cognitive human brain aging: a review. Gerontology 39, 280–303.

Lorenzo-López, L., Amenedo, E., Pazo-Álvarez, P., Cadaveira, F., 2007. Visual target processing in high- and low-performing older subjects indexed by P3 component. Neurophysiologie Clinique/Clinical Neurophysiology 37, 53–61.

McNair, S.W., Kayser, S.J., Kayser, C., 2019. Consistent pre-stimulus influences on auditory perception across the lifespan. NeuroImage 186, 22–32.

Miller, K.J., Sorensen, L.B., Ojemann, J.G., Nijs, den, M., 2009. Power-Law Scaling in the Brain Surface Electric Potential. PLoS Comput Biol 5, e1000609.

Mitchell, J.F., Sundberg, K.A., Reynolds, J.H., 2007. Differential attention-dependent response modulation across cell classes in macaque visual area V4. Neuron 55, 131–141.

Muthukumaraswamy, S.D., Liley, D.T., 2018. 1/f electrophysiological spectra in resting and drug-induced states can be explained by the dynamics of multiple oscillatory relaxation processes. NeuroImage 179, 582–595.

Peterson, E.J., Rosen, B.Q., Campbell, A.M., Belger, A., Voytek, B., 2018. 1/f neural noise is a better predictor of schizophrenia than neural oscillations. bioRxiv 113449.

Podvalny, E., Noy, N., Harel, M., Bickel, S., Chechik, G., Schroeder, C.E., Mehta, A.D., Tsodyks, M., Malach, R., 2015. A unifying principle underlying the extracellular field potential spectral responses in the human cortex. Journal of Neurophysiology 114, 505–519.

Pritchard, W.S., 2009. The Brain in Fractal Time: 1/F-Like Power Spectrum Scaling of the Human Electroencephalogram. International Journal of Neuroscience 66, 119–129.

Saville, C.W.N., Feige, B., Kluckert, C., Bender, S., Biscaldi, M., Berger, A., Fleischhaker, C., Henighausen, K., Klein, C., 2014. Increased reaction time variability in attention-deficit hyperactivity disorder as a response-related phenomenon: evidence from single-trial event-related potentials. J Child Psychol Psychiatr 56, 801–813.

Scholvinck, M.L., Saleem, A.B., Benucci, A., Harris, K.D., Carandini, M., 2015. Cortical State Determines Global Variability and Correlations in Visual Cortex. Journal of Neuroscience 35, 170–178.

Sheehan, T.C., Sreekumar, V., Inati, S.K., Zaghloul, K.A., 2018. Signal Complexity of Human Intracranial EEG Tracks Successful Associative-Memory Formation across Individuals. Journal of Neuroscience 38, 1744–1755.

Veerakumar, A., Tiruvadi, V., Howell, B., Waters, A.C., Crowell, A.L., Voytek, B., Riva-Posse, P., Denison, L., Rajendra, J.K., Edwards, J.A., Bijanki, K.R., Choi, K.S., Mayberg, H.S., 2019. Field potential 1/ factivity in the subcallosal cingulate region as a candidate signal for monitoring deep brain stimulation for treatment-resistant depression. Journal of Neurophysiology 122, 1023–1035.

Voytek, B., Knight, R.T., 2015. Dynamic Network Communication as a Unifying Neural Basis for Cognition, Development, Aging, and Disease. Biological Psychiatry 77, 1089–1097.

Voytek, B., Kramer, M.A., Case, J., Lepage, K.Q., Tempesta, Z.R., Knight, R.T., Gazzaley, A., 2015. Age-Related Changes in 1/f Neural Electrophysiological Noise. Journal of Neuroscience 35, 13257–13265.

Waschke, L., Wöstmann, M., Obleser, J., 2017. States and traits of neural irregularity in the age-varying human brain. Scientific Reports 7, 17381.

Yang, G.J., Murray, J.D., Repovs, G., Cole, M.W., Savic, A., Glasser, M.F., Pittenger, C., Krystal, J.H., Wang, X.J., Pearlson, G.D., Glahn, D.C., Anticevic, A., 2014. Altered global brain signal in schizophrenia. Proceedings of the National Academy of Sciences 111, 7438–7443.

CHAPTER 1: Alpha Phase Dynamics Predict Age-Related Visual Working Memory Decline

Abstract

Alpha oscillations (7-14 Hz) are modulated in response to visual temporal and spatial cues. However, the neural response to alerting cues is less explored, as is how this response is affected by healthy aging. Using scalp EEG, we examined how visual cortical alpha activity relates to working memory performance. Younger (20-30 years) and older (60-70 years) participants were presented with a visual alerting cue uninformative of the position or size of a lateralized working memory array. Older adults showed longer response times overall and reduced accuracy when memory load was high. Older adults had less consistent cue-evoked alpha phase resetting than younger adults, which predicted worse performance. Alpha phase prior to memory array presentation predicted response time, but the relationship between phase and response time was weaker in older adults. These results suggest that changes in alpha phase dynamics, especially prior to presentation of task-relevant stimuli, potentially contribute to age-related cognitive decline.

Introduction

In order to achieve high behavioral performance, limited attentional resources must be efficiently directed towards task-relevant information. Such information could include the timing or spatial position of upcoming visual stimuli. Knowledge of when (Nobre et al., 2007) or where (Posner, 1980) a target will appear enhances detection and shortens response times. Likewise, presentation of neutral warning cues improves

response times by heightening alertness or preparedness for upcoming stimuli. The effects of informative temporal and spatial cues are strongly related to the dynamics of 7-14-Hz alpha oscillations, as observed in anticipatory changes in alpha amplitude (Thut et al., 2006; van Diepen et al., 2015; Worden et al., 2000; Zanto et al., 2011) and phase (Samaha et al., 2015). How alpha dynamics are modulated in response to warning or alerting cues is less understood.

Neurologically healthy aging is associated with declines in attention and working memory. Behaviorally, the benefits of spatial cuing are relatively resistant to healthy aging (Hartley et al., 1992; Madden, 1990), but older adults derive less benefit from the presence of temporal (Zanto et al., 2011) and alerting cues (Gamboz et al., 2010; Jennings et al., 2007). Physiologically, older adults show reduced alpha modulation in response to temporal (Zanto et al., 2011) and spatial cues (Hong et al., 2015), though a recent study found no age-related differences in neural response to alerting cues (Williams et al., 2016). However, because alpha activity was not examined in that study, it is unclear whether older adults' reduced use of alerting cues can be predicted by concomitant changes in alpha oscillatory dynamics.

To investigate alpha response to alerting cues and how this response is affected by healthy aging, we recorded EEG from younger and older adults performing a unilateral visual working memory task. Each trial of the task included an alerting cue signaling the upcoming presentation of a lateralized memory array. This cue allowed us to probe participants' preparedness for upcoming stimuli independent of motor preparation. The alerting cue was uninformative of the size and location of the upcoming memory array, but was perfectly predictive of its timing. To favor bottom-up,

reflexive alerting over voluntary orienting or temporal expectation, the foreperiod between the cue and memory array was kept relatively short (Weinbach and Henik, 2012). We hypothesized that age-related changes in neural activity would manifest themselves in the alpha amplitude and phase response to presentations of the alerting cue. We also hypothesized that the extent to which neural response to the alerting cue was altered would also predict declines in working memory performance.

Materials and Methods

Behavioral Task

Healthy right-handed younger (20-30 year olds, *n* = 17, eight female) and older (60-70 year olds, *n* = 14, seven female) adults with normal or corrected-to-normal vision participated in a visual working memory paradigm. All participants gave informed consent approved by the UC Berkeley Committee on Human Research. In each trial, participants were instructed to maintain central fixation, and at the beginning of each trial, the central fixation cross flashed from gray to pink for 50 ms, alerting participants to the start of the upcoming trial (Figure 1.1A). This alerting cue offered no information on either the size or location of upcoming visual stimuli. Three hundred ms after the end of the alerting cue, participants were presented with one, two, or three colored squares for 180 ms in only one visual hemifield. After a 900 ms delay period, during which time no stimuli other than the fixation cross were present, a test array of the same number of squares in the same spatial locations appeared. Participants would manually respond with their right thumb to indicate whether or not the test array had the same color squares as the initial memory array.

Behavioral accuracy was assessed using *d′*, a sensitivity measure that takes false alarm and miss rates into account to correct for response bias. To avoid mathematical constraints in the calculation of *d′*, we applied a standard correction procedure in the case of 100% hit rate or 0% false alarm rate. Specifically, hit rate was decreased to 1 - 1/(2*N*) when necessary, with *N* being the total number of trials. Similarly, false alarm rate was increased to 1/(2*N*) when necessary (Macmillan and Creelman, 2004).

Data Acquisition

We recorded 64-channel scalp electroencephalography (EEG) from each participant. Participants were tested in a sound-attenuated EEG recording room using a 64+8 channel BioSemi ActiveTwo amplifier (Amsterdam, Netherlands). EEG was amplified (-3 dB at ~819 Hz low-pass, DC coupled), digitized (512 Hz), and stored for offline analysis. Horizontal eye movements (HEOG) were recorded with electrodes at both external canthi. Vertical eye movements (VEOG) were monitored with a left inferior eye electrode and either a superior eye or a fronto-polar electrode. All data was referenced offline to the average potential of two mastoid electrodes and analyzed in MATLAB® (R2015A, Natick, MA) using custom scripts and the EEGLAB toolbox (Delorme and Makeig, 2004).

Data Preprocessing

EEG data was downsampled to 256 Hz and had DC offset removed. EEG data was then highpass filtered above 0.1 Hz using a two-way, fourth-order Butterworth

infinite impulse response filter. Any channel whose standard deviation was ±2.5 standard deviations away from the mean standard deviation of all channels was spherically interpolated (on average, 2 channels per participant). Independent component analysis (ICA) was performed using the EEGLAB toolbox, and to remove blink artifacts, ICA components most correlated with the difference between the frontopolar and left inferior eye electrodes were removed.

For event-related potential (ERP) analyses and to detect trials with artifacts, continuous EEG data was lowpass filtered below 30 Hz using a two-way, fourth-order Butterworth infinite impulse response filter. Data was epoched around the onset of the memory array using a pre-stimulus baseline of -500 ms to -400 ms. For scalp topographic visualization, and to normalize electrode locations, electrode potentials were swapped right to left across the midline as though stimuli were always presented in the right visual hemifield, making left and right hemisphere channels contralateral and ipsilateral to the stimulus, respectively. Lateralized potentials were analyzed in this ipsilateral-contralateral fashion. Trials where the standard deviation of a scalp electrode exceeded three times the standard deviation of that electrode across all trials were excluded. For saccade trials, trials where the standard deviation of the difference between the HEOG channels exceeded three times the mean of the HEOG channels across all trials were excluded. On average, 69.6% of total trials or 165 trials were kept per participant. For younger adults, an average of 151 trials (minimum 21, maximum 364) per memory-load condition were included, and for older adults, an average of 182 trials (minimum 27, maximum 324) per memory-load condition were included. The

number of trials did not differ between younger and older adults (p = 0.23, Cohen's d = -0.44). No participants were excluded.

Data Analysis

P1 amplitudes were calculated as the average amplitude in a 50-ms window centered on participants' most positive local peak amplitude 80-180 ms after stimulus onset. Peak alpha frequency (PAF), the frequency of maximum power between 7 and 14 Hz, varies in a trait-like manner (Grandy et al., 2013) and predicts visual performance (Samaha and Postle, 2015). To estimate PAF for each participant, we constructed power spectral densities (PSDs) using Welch's method. In order to account for individual differences in 1/f electrophysiological background, which changes with age (Voytek et al., 2015a), we used robust linear regression to estimate and remove the slope and offset of log-log space PSDs prior to identification of PAF.

Continuous, non-lowpass-filtered EEG data was bandpass filtered with a 4-Hz passband centered on each participant's PAF. Filters were designed as two-way finite impulse response filters with filter length equal to three cycles of the low cutoff frequency. For each channel, bandpass-filtered time series were converted to z-scores using the mean and standard deviation of artifact-free alpha-band data across all trials and conditions. After normalization, the absolute value and angle of the Hilbert transform of the continuous EEG data was used to extract alpha analytic amplitudes and instantaneous phases, respectively. The phase time series yields cosine phase values of (-π, π] radians, with π radians corresponding to the trough and zero radians to

the peak of the oscillation. This method yields results equivalent to sliding-window fast Fourier transform and wavelet approaches (Bruns, 2004).

After epoching and removal of marked artifact trials, alpha analytic amplitude time series were subjected to event-related analyses, including the subtraction of baseline activity from -500 ms to -400 ms. To assess trial-to-trial phase consistency (also called intertrial coherence, ITC), event-related phase time series were extracted, and for each time point, the mean vector length of the timepoint's phase distribution was calculated across trials (*circ_r.m* function in the CircStats toolbox (Berens, 2009)). This mean vector length represents the degree of ITC, with ITC of unity reflecting a single adopted phase across trials and a value of zero reflecting uniformly distributed phases across trials.

Statistical Analyses

All analyses were performed on data from EEG channels O1/2, PO3/4, and PO7/8, with channels O1, PO3, and PO7 considered contralateral to the memory array. Multiple-factor statistical analyses were assessed via ANOVAs, with age as a between-group factor and memory load and hemisphere as within-group factors. Where sphericity assumptions were violated, degrees of freedom (and hence *p*-values) were adjusted using Greenhouse-Geisser corrections. All single-factor comparisons were analyzed via paired-samples or between-samples *t*-tests. For all alpha ITC analyses, ITC values were $\log_{10}$-transformed and baseline subtracted. To test for increases in ITC, each trial's phase time series was randomly scrambled, and null values of ITC were calculated using the scrambled trials. This procedure was repeated 1000 times per

memory load per participant, and a significant increase in ITC was considered as a true ITC value higher than the 97.5% percentile of the null ITC distributions. Peak cue- and array-related ITC were assessed using the maximum ITC peak after cue and memory array presentation, respectively. To correlate circular variables like alpha phase with linear variables like response time, a circular-linear correlation was used (*circ_corrcl.m* function in the CircStats toolbox).

Results

Behavior

Response Time

We compared younger and older adults' response times (RTs) on a lateralized visual working memory task (Figure 1.1a, see Methods). RTs showed main effects of age (Figure 1.1b, $F_{1,29} = 13.32$, $p = 0.0010$, generalized $\eta^2 = 0.31$) and memory load ($F_{2,58} = 67.20$, Greenhouse-Geisser (GG) $\varepsilon = 0.88$, $p_{GG} < 10^{-13}$, $\eta^2 = 0.089$) and an interaction between age and memory load ($F_{2,58} = 3.75$, $\varepsilon = 0.88$, $p_{GG} = 0.029$, $\eta^2 = 0.0054$). Between groups, younger adults had faster RTs than older adults in each load condition. This included load-one (541 ms vs. 643 ms, mean difference 95% confidence interval [-166 ms, -39 ms], $t_{28.91} = -3.29$, $p = 0.0027$, Cohen's $d = -1.17$), load-two (565 ms vs. 670 ms, [-166 ms, -44 ms], $t_{29} = -3.51$, $p = 0.0015$, Cohen's $d = -1.24$), and load-three conditions (591 ms vs. 721 ms, [-195 ms, -65 ms], $t_{29} = -4.09$, $p < 10^{-3}$, Cohen's $d = -1.45$).

Accuracy

As assessed using the sensitivity measure *d'*, accuracy showed an effect of memory load (Figure 1.1c, $F_{2,58} = 51.04$, $\varepsilon = 0.92$, $p_{GG} < 10^{-11}$, $\eta^2 = 0.16$) and an interaction between age and memory load ($F_{2,58} = 5.78$, $\varepsilon = 0.83$, $p_{GG} = 0.0065$, $\eta^2 = 0.021$). Accuracy was comparable between younger and older adults in load-one ($p = 0.73$, Cohen's $d = 0.13$) and load-two conditions ($p = 0.22$, Cohen's $d = 0.45$). However, younger adults outperformed older adults in load-three conditions (3.32 vs. 2.58, [0.042, 1.45], $t_{29.00} = 2.17$, $p = 0.039$, Cohen's $d = 0.77$). In summary, older adults showed slower RTs overall and reduced working memory accuracy specifically during high-load trials.

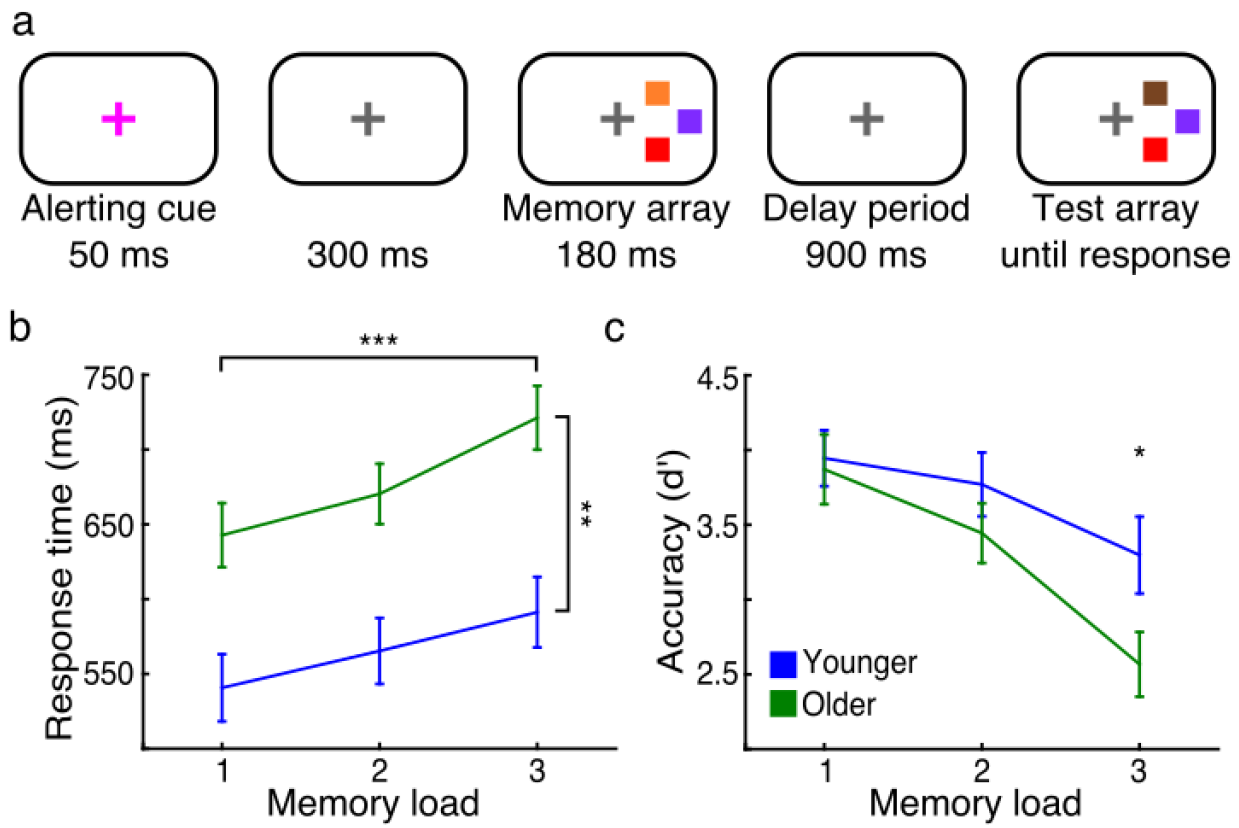

Figure 1.1. Paradigm and behavioral performance. (*a*) Diagram of the task design, in this example showing a non-matching test array. (*b*) Response times increased with increasing memory load, with younger adults (blue) faster than older adults (green, $^{**}p < 0.01$, $^{***}p < 0.001$; error bars, SEM). (*c*) Accuracy decreased with increasing memory load, with younger adults more accurate than older adults during load-three trials ($^{*}p < 0.05$; age by memory load interaction: $p < 0.01$; error bars, SEM).

EEG

Alerting Cue Activity

To investigate neurophysiological measures potentially underlying decreased behavioral performance in older adults, we first examined younger and older adults' neural response to presentations of the alerting cue. During task performance, younger and older adults exhibited 7-14 Hz oscillatory alpha activity in visual parietal-occipital regions (Figure 1.2a). Based on participants' peak alpha frequency, previously shown to be lower in older adults[14], we determined individualized alpha bands and compared participants' normalized alpha analytic amplitude and instantaneous phase activity during the task. To also examine the consistency in alpha phase activity across trials, we computed alpha intertrial coherence (ITC) per participant.

Parietal-occipital visual regions showed alpha amplitude and ITC response to presentations of the alerting cue (Figure 1.2b, Figure 1.2c). Alpha amplitude modulation in response to the alerting cue (-350 to 0 ms) showed no effects of age ($F_{1,29}$ = 2.82, p = 0.10, η^2 = 0.074), hemisphere ($F_{1,29}$ < 1.0), or memory load ($F_{2,58}$ < 1.0). This lack of hemisphere and memory load effect is consistent with the alerting cue being uninformative of the lateral position or number of upcoming stimuli.

Compared to baseline (-500 to -350 ms), average alpha ITC increased in response to the alerting cue in younger adults (Figure 1.2c, [-0.56, -0.29], t_{16} = -6.73, p < 10^{-5}, Cohen's d = -1.63) and weakly in older adults ([-0.14, 0.011], t_{13} = -1.83, p = 0.090, Cohen's d = -0.49). As compared to ITC values calculated using phase-scrambled trials, true average cue-evoked (-350 to 0 ms) ITC was higher in 17 of 17 younger adults as well as 11 of 14 older adults. Peak cue-evoked ITC occurred on

average 207 and 185 ms after alerting cue onset in younger and older adults, respectively, with peak ITC latency comparable between younger and older adults (p = 0.39, Cohen's d = 0.34). These increases in ITC suggest the presence of stimulus-evoked alpha phase resets in both younger and older adults. As with alpha amplitude, peak cue-evoked ITC did not show an effect of hemisphere ($F_{1,29} < 1.0$) or memory load ($F_{2,58} < 1.0$), again consistent with the noninformative nature of the alerting cue. However, younger adults had higher peak cue-evoked ITC than did older adults (Figure 1.3a, Figure 1.3b, 0.63 vs. 0.23, [0.24, 0.56], $F_{1,29} = 23.64$, $p < 10^{-4}$, $\eta^2 = 0.32$). There was also no age-related difference in cue-evoked P1 amplitude (p = 0.24, Cohen's d = 0.40).

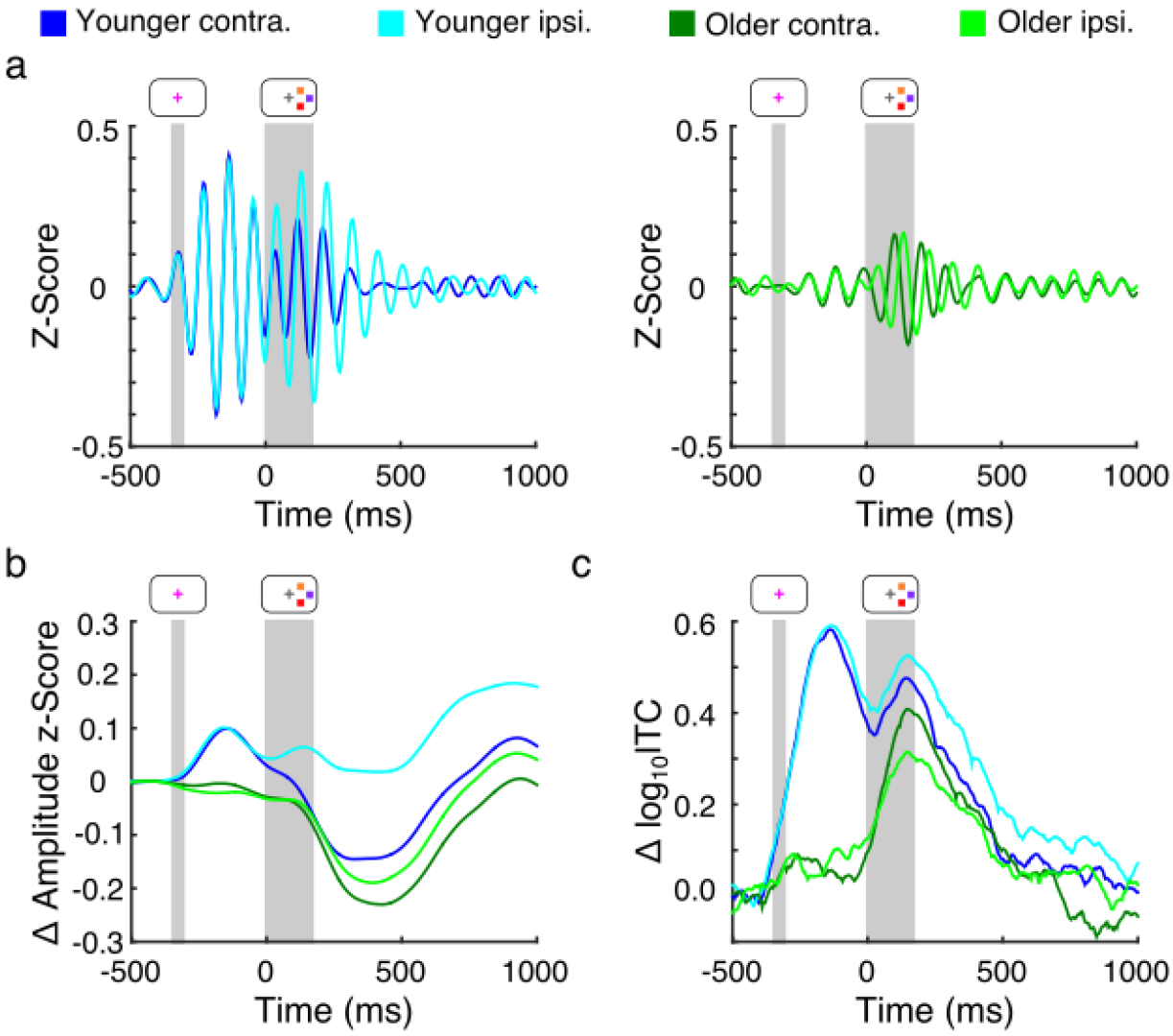

Figure 1.2. Alpha amplitude and phase activity. (a) Grand average visual-area alpha activity contralateral (darker) and ipsilateral (lighter) to the memory array in younger (blue, left panel) and older adults (green, right panel). Gray regions indicate presence and duration of the alerting cue and memory array. Note the hemispheric amplitude differences and strong phase consistency in younger compared to older adults. (*b*) Grand average of changes in normalized visual-area alpha amplitude and (*c*) intertrial coherence relative to baseline, emphasizing the effects observable in (*a*).

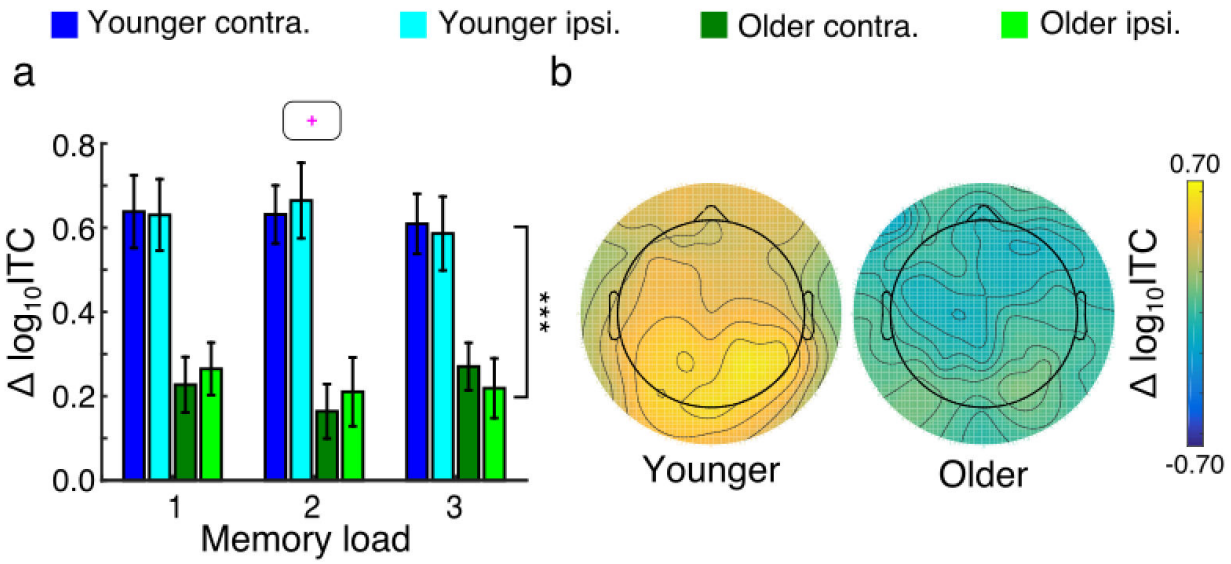

Figure 1.3. Alerting cue activity. (*a*) Peak alpha intertrial coherence (ITC) in response to the alerting cue. Younger adults (blue) had higher peak cue-evoked ITC than older adults (green; ***$p < 0.001$; error bars, SEM). (*b*) Topographies of cue-evoked ITC response in younger (left) and older adults (right) during load-three trials.

Memory Array Activity

Younger and older adults also showed alpha response to presentation of the memory array. After memory array onset, alpha amplitude diverged between hemispheres in younger and older adults (Figure 1.2b). Mean alpha amplitude (0 to 400 ms) showed main effects of memory load (Figure 1.4a, Figure 1.4b, $F_{2,58} = 4.29$, $\varepsilon = 0.87$, $p_{GG} = 0.024$, $\eta^2 = 0.011$) and hemisphere ($F_{1,29} = 18.15$, $p < 10^{-3}$, $\eta^2 = 0.034$) and an interaction between age and hemisphere ($F_{1,29} = 9.10$, $p = 0.0053$, $\eta^2 = 0.017$). Post hoc analysis revealed that alpha amplitude decreased from load-one to load-two ([0.0053, 0.056], $t_{30} = 2.47$, $p = 0.019$, Cohen's $d = 0.44$), but not from load-two to load-three conditions ($p = 0.37$, Cohen's $d = 0.17$). In addition, alpha lateralization, or the difference in alpha amplitude between hemispheres, was greater in younger than older adults (0.11 vs. 0.019, [0.034, 0.15], $t_{23.21} = 3.22$, $p = 0.0038$, Cohen's $d = 1.09$).

As with alerting cue presentation, memory array presentation also caused alpha phase resets (Figure 1.2c). Overall, both younger ([-0.43, -0.18], $t_{16} = -5.27$, $p < 10^{-4}$, Cohen's $d = -1.28$) and older adults ([-0.30, -0.099], $t_{13} = -4.25$, $p < 10^{-4}$, Cohen's $d = -1.14$) showed increased average alpha ITC in response to the memory array. Compared to phase-scrambled ITC values, true average array-evoked (0 to 600 ms) ITC was higher in all 17 younger adults and all 14 older adults. Unlike with cue-evoked ITC, peak array-evoked ITC showed no effects of memory load ($F_{2,58} < 1.0$), age ($F_{1,29} = 1.60$, $p = 0.22$, $\eta^2 = 0.028$), or hemisphere ($F_{1,29} < 1.0$).

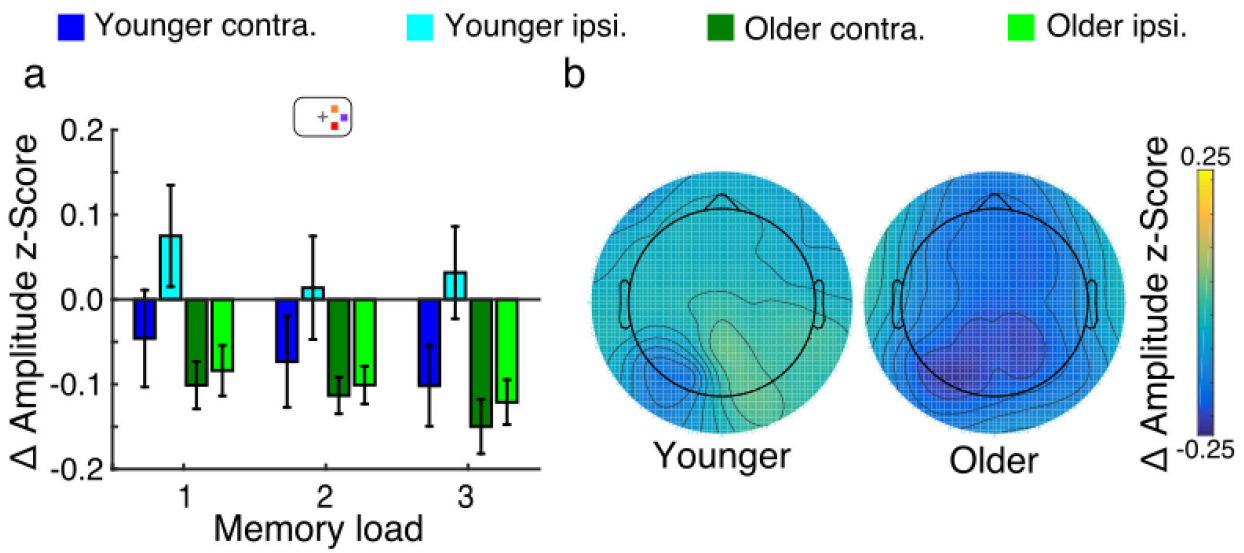

Figure 1.4. Memory array activity. (*a*) Average change relative to baseline in normalized alpha amplitude 0 to 400 ms after memory array presentation. Amplitude decreased from load one to two ($p < 0.05$), and older adults (green) showed decreased alpha lateralization ($p < 0.01$; error bars, SEM). (*b*) Topographies of delay-period alpha amplitude in younger (left) and older adults (right) during load-three trials.

Contralateral Delay Activity

We also investigated participants' contralateral delay activity (CDA), an event-related potential measure indicative of working memory capacity (McCollough et al., 2007; Vogel and Machizawa, 2004) and top-down attentional processes (Drew and Vogel, 2008; Eimer and Kiss, 2010; Fukuda and Vogel, 2009; Woodman and Vogel, 2008). We observed sustained delay-period (300 to 900 ms) negativity in the hemisphere contralateral to the memory array (Figure 1.5a). This negativity or CDA showed a main effect of memory load (Figure 1.5b, $F_{2,58} = 14.88$, $\varepsilon = 0.96$, $p_{GG} < 10^{-5}$, $\eta^2 = 0.080$) wherein CDA increased in magnitude from load-one to load-two conditions ([0.34 μV, 0.86 μV], $t_{30} = 4.66$, $p < 10^{-4}$, Cohen's $d = 0.84$). CDA was comparable between load-two and load-three conditions ($p = 0.47$, Cohen's $d = 0.13$). However, CDA did not differ between younger and older adults ($F_{1,29} = 1.05$, $p = 0.31$, $\eta^2 = 0.029$), nor did we observe an interaction between age and memory load ($F_{2,58} < 1.0$).

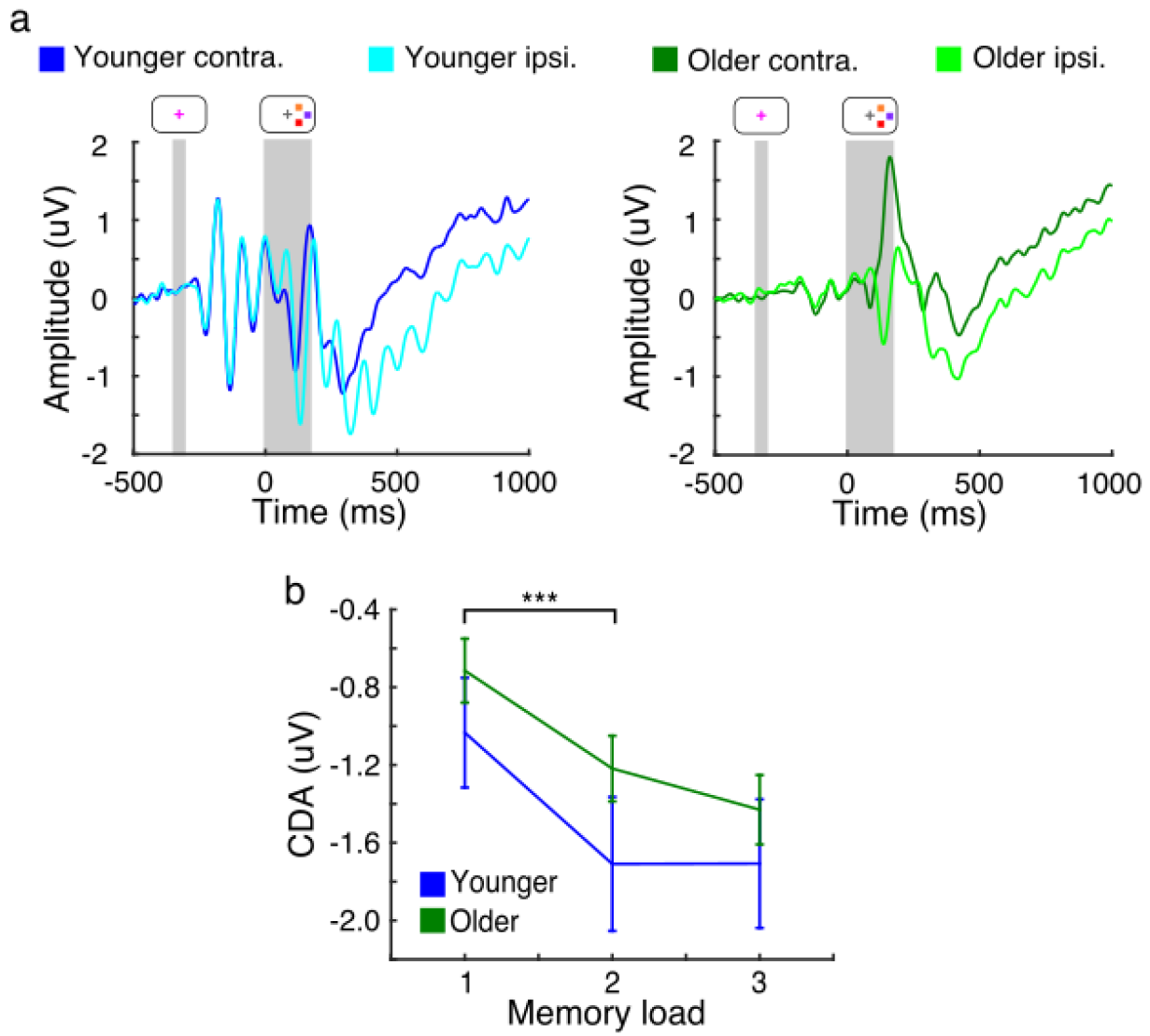

Figure 1.5. Event-related potential and delay period activity. (*a*) Grand average visual-area activity contralateral (darker) and ipsilateral (lighter) to the memory array in younger (left panel) and older adults (right panel). Gray regions indicate presence and duration of the alerting cue and memory array. Note the sustained negativity in the contralateral hemisphere in both younger and older adults. (*b*) Contralateral delay activity (CDA) increased in magnitude from load-one to load-two conditions, but did not differ between younger and older adults (***$p < 0.001$; error bars, SEM)

Alpha Phase Activity Predicts Behavior

Given the age-related changes in neural activity that we observed, we examined how these changes related to behavioral performance. As noted, older adults performed as well as younger adults on the easiest (load-one and load-two) trials, but performed worse for more difficult load-three trials. To examine the neurophysiological basis for this aging effect, we focused our analyses on measures of cue-evoked alpha ITC, array-evoked alpha amplitude modulation, and delay-period CDA. Peak cue-evoked ITC was averaged across visual hemispheres, and the differences in alpha lateralization and CDA between load-two and load-three conditions were used. Importantly, these physiological measures were indexed during times *prior to* the actual memory challenge and thus are related to trial-by-trial changes in alertness, encoding, or memory maintenance, rather than memory retrieval or response.

Across all participants, between-load differences in alpha lateralization were not predictive of load-three accuracy ($N = 31$, $p = 0.45$), nor were between-load differences in alpha lateralization and CDA correlated with one another ($N = 31$, $p = 0.85$). Similar to previous results (Vogel and Machizawa, 2004), between-load differences in CDA were predictive of load-three accuracy ($N = 31$, $r = -0.41$, $p = 0.022$). This effect was driven by a correlation across younger adults alone ($N = 17$, Spearman's $r = -0.65$, $p = 0.0048$), with no such correlation among older adults ($p = 0.42$). Peak cue-evoked ITC was also correlated with load-three accuracy across all participants (Figure 1.6a; $N = 31$, Spearman's $r = 0.47$, $p = 0.0071$). As with CDA effects, this was driven by a correlation across younger adults alone ($N = 17$, Spearman's $r = 0.49$, $p = 0.044$), with no such correlation among older adults ($p = 0.62$).

Next, to examine the relative contribution of each neurophysiological measure to behavioral accuracy, we modeled load-three *d′* as a linear combination of load-three peak cue-evoked alpha ITC and the between-load differences in array-evoked alpha lateralization and delay-period CDA. This model explained 18.5% of the variance in accuracy ($p = 0.036$). Examining the relative contribution of each predictor, we found that after accounting for between-load differences in alpha lateralization and CDA, peak cue-evoked ITC remained predictive of load-three accuracy ($p = 0.025$). Between-load differences in alpha lateralization and CDA, on the other hand, did not remain predictive of load-three accuracy after accounting for other physiological measures ($p = 0.70$ and $p = 0.22$, respectively). Thus, peak cue-evoked ITC prior to the presentation of to-be-remembered stimuli was a strong predictor of behavioral accuracy, even after adjusting for array-related alpha amplitude and delay-period CDA effects.

To further investigate how cue-evoked alpha ITC is associated with behavioral performance, we examined how alpha phase at peak ITC related to subsequent working memory performance. To do so, we determined the timepoint of each participant's peak cue-evoked ITC, and we pooled all participants' corresponding alpha phases at peak cue-evoked ITC and RTs across trials. During load-three trials in younger adults, alpha phase at peak cue-evoked ITC predicted RTs on a trial-by-trial basis (Figure 1.6b, blue; $N = 2499$, $r = 0.13$, $p < 10^{-3}$). Alpha phase at peak cue-evoked ITC also predicted RTs in older adults (Figure 1.6B, green; $N = 2090$, $r = 0.080$, $p = 0.0013$). Specifically, in both younger and older adults, longer response times were predicted by peak cue-evoked ITC occurring at the peak of the alpha cycle. Thus, despite older adults' relatively inconsistent cue-evoked phase response, prestimulus alpha phase was still

predictive of load-three RTs. However, the relationship between alpha phase at peak cue-evoked ITC and RT was weaker in older than younger adults (z = 1.79, p = 0.036), indicating a weaker prestimulus alpha phase effect among older adults.

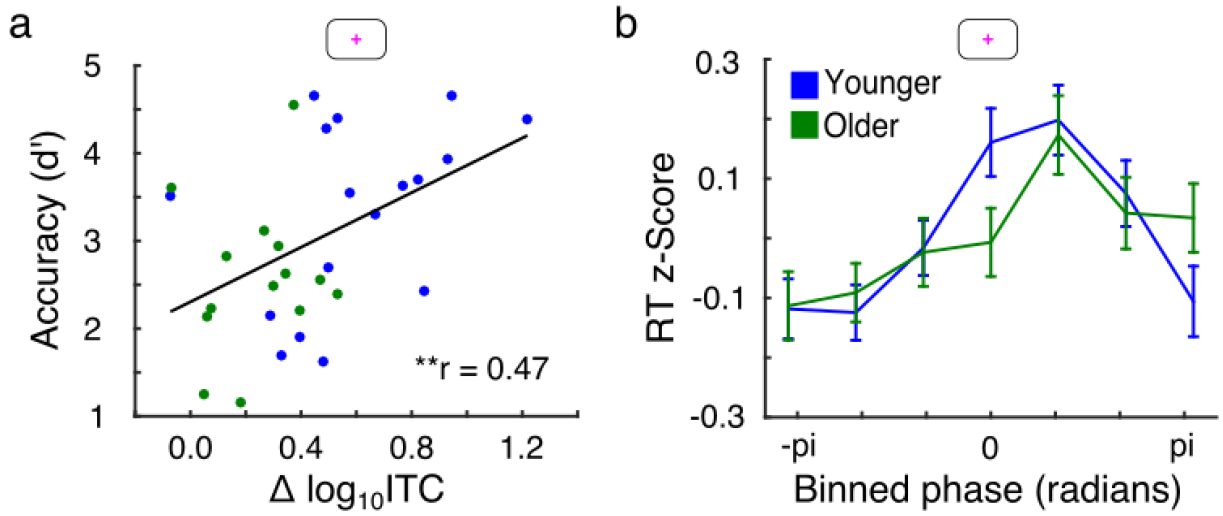

Figure 1.6. Alpha phase predicts working memory performance. (*A*) Peak cue-evoked alpha intertrial coherence (ITC) versus accuracy during load-three trials across younger (blue) and older adults (green). Peak cue-evoked ITC was predictive of load-three accuracy (**$p < 0.01$). (*B*) Average response time (RT) binned by alpha phase at peak cue-evoked ITC. Phase of zero and ±pi correspond to the peaks and troughs of alpha, respectively. Trial-by-trial alpha phase predicted RTs ($p < 10^{-3}$; error bars, SEM).

Discussion

In this study, we used a combined visual attention and working memory task to investigate how age-related changes in alertness and spatial attention affect later working memory performance. Using scalp EEG, we found that alpha activity showed age-related alterations during the task, including in older adults' reduced alpha amplitude lateralization during working memory maintenance. In addition, prior to working memory encoding, older participants showed less consistent phase response to a spatially noninformative alerting cue. The consistency of cue-evoked alpha phase reset predicted working memory performance, as did prestimulus alpha phase prior to memory array presentation. Our results provide evidence that alerting cue presentation is accompanied by alpha activity modulation, that neural response to alerting cues is altered during healthy aging, and that the degree of alteration could influence behavioral outcomes.

Previous research has found that contralateral delay activity (CDA) is related to reduced working memory performance in older frontal and basal ganglia lesion patient populations (Voytek et al., 2010; Voytek and Knight, 2010). In this study, we observed that between-load modulation of CDA predicted working memory performance, which is consistent with previous findings (Vogel and Machizawa, 2004). We observed no difference in the amplitude or load-dependent modulation of CDA between younger and older adults. A previous study has reported alterations in CDA modulation in older adults (Sander et al., 2011), but differences between that study and our present study are likely due to our study only presenting stimuli in one visual hemifield at a time. Thus,

any age-related differences in the suppression of distractor processing were not tested, likely altering patterns of CDA modulation in older adults.

After memory array presentation, alpha amplitude in younger adults diverged between hemispheres, with ipsilateral amplitude higher than contralateral amplitude. Consistent with previous studies (Thut et al., 2006; Worden et al., 2000), this alpha lateralization is suggestive of differential processing of the two visual hemifields and the deployment of selective spatial attention in anticipation of the test array, which participants knew would appear in the same visual hemifield as the memory array. This interpretation is also consistent with the lack of alpha lateralization in response to the spatially uninformative alerting cue. Compared to younger adults, older adults showed reduced alpha lateralization, as previously reported in studies with spatial cuing (Hong et al., 2015; Sander et al., 2012). However, between-load modulation of alpha lateralization did not predict older adults' lower accuracy during load-three trials.

Instead, cue-evoked alpha phase resetting was less consistent in older adults and was predictive of behavioral performance even after adjusting for array-evoked alpha lateralization and delay-period CDA. Because the alerting cue appeared prior to any stimulus to be encoded in working memory, this result supports findings of reduced alertness in older adults (Gamboz et al., 2010; Jennings et al., 2007), with participants' general attentional state being the single best predictor of accuracy more than a second later in the trial. Because the alerting cue was also temporally predictive and preceded memory array onset by 300 ms each trial, these results are similar to those of Zanto *et al*. (2011), which showed that older adults had reduced pre-target alpha activity modulation during a 600 ms foreperiod. Our results extend these previous findings

because of our use of a shorter foreperiod designed to test alerting over orienting response (Weinbach and Henik, 2012). Thus, while Zanto *et al*. (2011) demonstrated age-related reductions in neural measures of temporal expectation, our results highlight older adults' reduced reflexive response instead.

Although the observed age-related differences in cue-evoked ITC are consistent with previous reports of reduced alertness in older adults (Gamboz et al., 2010; Jennings et al., 2007), age-related changes in early perceptual processing could also have contributed to the observed effects, especially given the briefness of alerting cue presentation (50 ms). However, younger and older adults had comparable cue-evoked P1 amplitudes, suggesting that both groups visually processed the cue in a similar manner. If this were not the case, lower performance in older adults would potentially be more attributable to changes in visual processing than to changes in alerting response. Nevertheless, although we did not observe any changes in cue-evoked P1 amplitude, differences in perceptual processing cannot be ruled out as a potential factor contributing to age-related changes in working memory performance.

While the age-related inconsistency in cue-evoked alpha phase resetting is opposite that in a previous study (Sander et al., 2012), this discrepancy could be due to the lack of distractor stimuli and the briefness with which we presented the alerting cue (50 ms). This briefness potentially exacerbated any age-related alterations in cue response, which has not been observed in other studies (Williams et al., 2016; Zanto et al., 2011). Interestingly, we also found that array-evoked ITC was similar between younger and older adults, despite previous reports showing increased ITC among older adults (Sander et al., 2012). However, the large, asymmetric cue-evoked ITC

differences between younger and older adults may have shifted the ITC baseline, artificially driving up younger-adult ITC. That is, the peak-to-peak difference between cue- and array-evoked ITC is much larger among older, compared to younger, adults. Nevertheless, that cue-evoked alpha phase consistency was predictive of behavioral performance is consistent with previous studies examining alpha phase resetting in response to task-relevant stimuli (Klimesch et al., 2004; Werkle-Bergner et al., 2012; Yamagishi et al., 2008). Our results extend these findings by demonstrating that alpha phase resetting in response to alerting cues, even prior to presentation of to-be-remembered stimuli, can predict subsequent working memory performance.

Alpha phase prior to memory array presentation also predicted response time in high-load trials. This result provides further evidence for the effects of alpha phase on visual working memory (Myers et al., 2014). These effects have also been demonstrated in visual detection paradigms (Busch and VanRullen, 2010; Mathewson et al., 2009). Due to the consistent time interval between cue and memory array presentation in our study, it is possible that cue-evoked alpha phase resets led to subsequent memory array presentation at phases facilitative of or detrimental to perception or encoding of the memory array. Older adults' inconsistency in phase response could have led to a greater number of instances in which memory array presentation occurred at suboptimal alpha phases, potentially explaining part of the age-related reductions in performance we observed during high-load trials. However, older adults' weaker relationship between alpha phase and response time also suggests age-related reductions in the influence of alpha phase on visual cognition. Physiologically, this reduced influence, as well as older adults' inconsistent cue-evoked

phase responses, may relate to age-related increases in neural noise (Voytek and Knight, 2015; Voytek et al., 2015b).

Conclusions

Overall, we find that oscillatory alpha dynamics may underlie age-related alterations in attention. Our analysis of alpha phase highlights reductions in older adults' response and attentiveness to alerting cues, with such responsiveness being the strongest predictor of working memory performance. In addition, prestimulus alpha phase predicted performance on a trial-by-trial basis, but less reliably so in older adults. Given that lower performance in older adults can be explained by altered response to alerting cues prior to the task, age-related working memory decline is likely multifaceted and includes alterations in anticipatory attentional allocation as well as in stimulus encoding and maintenance. These findings suggest that changes in neural response, especially in older adults, can occur at multiple timepoints both before and after presentation of task-relevant stimuli, and such alterations likely all have an impact on later cognitive performance.

Chapter 1, in full, is a reprint of the material as it appears in: Tran, T. T., Hoffner, N. C., LaHue, S. C., Tseng, L. & Voytek, B. Alpha phase dynamics predict age-related visual working memory decline. NeuroImage 143, 196–203 (2016). The dissertation author was the primary investigator and author of this paper.

References

Berens, P., 2009. CircStat: a MATLAB toolbox for circular statistics 31.

Bruns, A., 2004. Fourier-, Hilbert- and wavelet-based signal analysis: are they really different approaches? Journal of Neuroscience Methods 137, 321–332.

Busch, N.A., VanRullen, R., 2010. Spontaneous EEG oscillations reveal periodic sampling of visual attention. Proc. Natl. Acad. Sci. U.S.A. 107, 16048–16053.

Delorme, A., Makeig, S., 2004. EEGLAB: an open source toolbox for analysis of single-trial EEG dynamics including independent component analysis. Journal of Neuroscience Methods 134, 9–21.

Drew, T., Vogel, E.K., 2008. Neural Measures of Individual Differences in Selecting and Tracking Multiple Moving Objects. Journal of Neuroscience 28, 4183–4191.

Eimer, M., Kiss, M., 2010. An electrophysiological measure of access to representations in visual working memory. Psychophysiol 47, 197–200.

Fukuda, K., Vogel, E.K., 2009. Human Variation in Overriding Attentional Capture. Journal of Neuroscience 29, 8726–8733.

Gamboz, N., Zamarian, S., Cavallero, C., 2010. Age-Related Differences in the Attention Network Test (ANT). Experimental Aging Research 36, 287–305.

Grandy, T.H., Werkle-Bergner, M., Chicherio, C., Lövdén, M., Schmiedek, F., Lindenberger, U., 2013. Individual alpha peak frequency is related to latent factors of general cognitive abilities. NeuroImage 79, 10–18.

Hartley, A.A., Kieley, J., McKenzie, C.R., 1992. Allocation of visual attention in younger and older adults. Percept Psychophys 52, 175–185.

Hong, X., Sun, J., Bengson, J.J., Mangun, G.R., Tong, S., 2015. Normal aging selectively diminishes alpha lateralization in visual spatial attention. NeuroImage 106, 353–363.

Jennings, J.M., Dagenbach, D., Engle, C.M., Funke, L.J., 2007. Age-Related Changes and the Attention Network Task: An Examination of Alerting, Orienting, and Executive Function. Aging, Neuropsychology, and Cognition 14, 353–369.

Klimesch, W., Schack, B., Schabus, M., Doppelmayr, M., Gruber, W., Sauseng, P., 2004. Phase-locked alpha and theta oscillations generate the P1–N1 complex and are related to memory performance. Cognitive Brain Research 19, 302–316.

Macmillan, N.A., Creelman, C.D., 2004. Detection Theory: A User's Guide, 2nd ed. Psychology Press, New York.

Madden, D.J., 1990. Adult age differences in attentional selectivity and capacity. European Journal of Cognitive Psychology 2, 229–252.

Mathewson, K.E., Gratton, G., Fabiani, M., Beck, D.M., Ro, T., 2009. To See or Not to See: Prestimulus Alpha Phase Predicts Visual Awareness. Journal of Neuroscience 29, 2725–2732.

McCollough, A.W., Machizawa, M.G., Vogel, E.K., 2007. Electrophysiological Measures of Maintaining Representations in Visual Working Memory. Cortex 43, 77–94.

Myers, N.E., Stokes, M.G., Walther, L., Nobre, A.C., 2014. Oscillatory Brain State Predicts Variability in Working Memory. Journal of Neuroscience 34, 7735–7743.

Nobre, A.C., Correa, A., Coull, J.T., 2007. The hazards of time. Current Opinion in Neurobiology 17, 465–470.

Posner, M.I., 1980. Orienting of attention. Quarterly Journal of Experimental Psychology 32, 3–25.

Samaha, J., Bauer, P., Cimaroli, S., Postle, B.R., 2015. Top-down control of the phase of alpha-band oscillations as a mechanism for temporal prediction. Proc. Natl. Acad. Sci. U.S.A. 112, 8439–8444.

Samaha, J., Postle, B.R., 2015. The Speed of Alpha-Band Oscillations Predicts the Temporal Resolution of Visual Perception. Current Biology 25, 2985–2990.

Sander, M.C., Werkle-Bergner, M., Lindenberger, U., 2012. Amplitude modulations and inter-trial phase stability of alpha-oscillations differentially reflect working memory constraints across the lifespan. NeuroImage 59, 646–654.

Sander, M.C., Werkle-Bergner, M., Lindenberger, U., 2011. Contralateral Delay Activity Reveals Life-Span Age Differences in Top-Down Modulation of Working Memory Contents. Cerebral Cortex 21, 2809–2819.

Thut, G., Nietzel, A., Brandt, S.A., Pascual-Leone, A., 2006. Alpha-Band Electroencephalographic Activity over Occipital Cortex Indexes Visuospatial Attention Bias and Predicts Visual Target Detection. Journal of Neuroscience 26, 9494–9502.

van Diepen, R.M., Cohen, M.X., Denys, D., Mazaheri, A., 2015. Attention and Temporal Expectations Modulate Power, Not Phase, of Ongoing Alpha Oscillations. Journal of Cognitive Neuroscience 27, 1573–1586.

Vogel, E.K., Machizawa, M.G., 2004. Neural activity predicts individual differences in visual working memory capacity. Nature 428, 748–751.

Voytek, B., Davis, M., Yago, E., Barceló, F., Vogel, E.K., Knight, R.T., 2010. Dynamic Neuroplasticity after Human Prefrontal Cortex Damage. Neuron 68, 401–408.

CHAPTER 2: Linked sources of neural noise contribute to age-related cognitive decline

Abstract

Healthy aging is associated with a multitude of structural changes in the brain. These physical age-related changes are accompanied by increased variability in neural activity of all kinds, and this increased variability, collectively referred to as "neural noise," is argued to contribute to age-related cognitive decline. In this study, we examine the relationship between two particular types of neural noise in aging. We recorded scalp EEG from younger (20-30 years) and older (60-70 years) adults performing a spatial visual discrimination task. First, we used the 1/*f*-like slope of the EEG power spectrum, a putative marker of excitation-inhibition balance, to assess baseline shifts toward a more excitatory, noisy state in aging. Next, we examined age-related decreases in the trial-by-trial consistency of visual stimulus processing. Finally, we examined to what extent these two age-related noise markers are related, hypothesizing that greater baseline noise would increase the variability of stimulus-evoked responses. We found that visual cortical baseline noise was higher in older adults, and the consistency of older adults' oscillatory alpha (8-12 Hz) phase responses to visual targets was also lower than that of younger adults. Crucially, older adults with the highest levels of baseline noise also had the least consistent alpha phase responses, while younger adults with more consistent phase responses achieved better behavioral performance. These results establish a link between tonic neural noise and stimulus-associated neural variability in aging. Moreover, they suggest that tonic age-related increases in baseline noise might diminish sensory processing and, as a result, subsequent cognitive performance.

Significance Statement

Neural noise, or variability in neural activity, increases with age. Using EEG, we examined two such age-related changes in neural noise and how they relate to behavioral performance. One change we examined was an age-related shift in baseline or non-stimulus-evoked activity towards a noisier, desynchronized state. The other was a decrease in the trial-by-trial consistency of sensory processing. We found that older adults with higher baseline noise had less consistent stimulus-evoked responses, whereas younger adults with the most consistent evoked responses had better behavioral performance. These results link two age-related changes in neural noise, suggest that tonic alterations in baseline activity might impact sensory processing, and highlight the need for understanding more about ongoing activity's effect on behavioral performance.

Introduction

Neural activity fluctuates over time even in the absence of external stimuli (Faisal et al., 2008; Dinstein et al., 2015). Such variability is seen at all measurement scales, from single-unit spiking to the fMRI BOLD signal, and is present both at rest and across repeated trials. These kinds of variability are collectively referred to as "noise" and are variously linked to numerous neurological disorders as well as decreased cognitive performance. Recent studies have begun to operationalize one aspect of noise using a signal processing definition based on the shape of the power spectrum of the encephalographic (EEG) signal (Voytek et al., 2015; Voytek & Knight 2015). By definition, white noise is a purely stochastic signal with a "flat" power spectrum (equal

power at all frequencies), whereas neural activity is 1/*f*-like in that power deceases exponentially as a function of frequency (Miller et al., 2009; He, 2014). The rate of this spectral power decrease—the slope of the 1/*f*-like power spectrum in log-log space—indexes the statistical structure of neural activity in that less negative or flatter slope indicates decorrelated, more-white-noise-like signals (Voytek et al., 2015; Voytek & Knight 2015; Gao, 2015). In addition, 1/*f*-like slope has also been shown to index the excitation-inhibition (EI) balance of the underlying neural population (Gao et al., 2017). In this EI framing, a flatter slope suggests a shift away from inhibition and toward "noisier" or more stochastic excitatory spiking.

In support of the neural noise hypothesis of aging, which proposes that healthy aging leads to diminished signal-to-noise in neural communication (Cremer and Zeef, 1987, Voytek & Knight, 2015), recent studies have shown age-related increases in EEG 1/*f*-like noise and how these changes relate to alterations in cognitive performance (Voytek et al., 2015, Waschke et al., 2017; McNair et al., 2018). Potentially reflecting increased EI balance, these increases in baseline noise would be consistent with reported reduced inhibitory signaling in aging (Hickmott and Dinse, 2013). Additionally, the consistency of activity evoked by identical or near-identical stimuli, which is already highly variable across trials (Scholvinck et al., 2015), has also been found to be reduced in older adults. For instance, the amplitude and latency of various visual event-related potential (ERP) components can, depending on electrode locations and stimulus paradigms, be more variable in older adults (Kugler et al., 1993; Lorenzo-Lopez et al., 2007). Similarly, decreases in the consistency of stimulus-evoked oscillatory alpha (roughly 8-12 Hz) phase responses, measured using intertrial phase coherence (ITC),

have also been reported (Tran et al., 2016, though see Sander et al., 2012, and Wiegand and Sander, 2019). Given concomitant age-related increases in baseline noise and response variability, it is possible that more prominent baseline noise might have a direct effect on the consistency with which older adults respond to and process external stimuli.

Here, we investigate the relationship between these two kinds of neural noise—tonic baseline noise and trial-by-trial response variability—as well as their association with age-related cognitive decline. To do so, we recorded EEG from younger (20-30 years) and older (60-70 years) adults performing a spatial visual discrimination task (Rolle et al., 2015, Rolle et al., 2017, Voytek et al., 2017). To assess baseline noise, the 1/*f*-like power spectrum slope of pre-trial visual posterior neural activity was used. To estimate response variability, we measured the increase in oscillatory alpha ITC evoked by visual target presentation. We hypothesized that older adults would have higher levels of baseline noise and higher response variability than would younger adults, and that older adults with higher levels of baseline noise would also have higher variability in stimulus-evoked responses.

Materials and Methods

Behavioral Task

All participants gave informed consent in accordance with protocols approved by the UCSF Committee on Human Research in the Human Research Protection Program. Healthy right-handed younger (20-30 years old) and older (60-70 years old) adults with normal or corrected-to-normal vision participated in a previously described visual

discrimination task (Rolle et al., 2015, Rolle et al., 2017, Voytek et al., 2017). In this task, a modified Posner attentional cueing task, we parametrically manipulated the amount of spatial information provided by a pre-target visual cue, in doing so instructing participants to focus or divide their attention across narrow or broad areas of visual space (Figure 2.1A). Each trial consisted of spatial cue presentation (100 ms), a preparatory period (1500-2000 ms, uniformly distributed, central fixation cross on-screen), and simultaneous visual target and non-target presentation (50 ms).

The spatial cue consisted of a green- and red-checkered circle surrounding the fixation cross, color luminances being matched. The circle was bisected along the vertical meridian with a black line. For the 100% certainty condition, the checkerboard was broken along the horizontal meridian by a solid red line in one hemifield and a solid green line in the other hemifield. These lines were the same vertical width as the arms of the fixation cross, and they extended the entire radius of the cue circle. In this condition, the hemifield of the green line was perfectly informative of the upcoming target location, which would appear 4.5° away from center exactly on the horizontal meridian in the green-line hemifield. For the 75% certainty condition, the cue instead had green and red 90° wedges centered along the horizontal meridian. In this condition, the hemifield of the green wedge was still perfectly informative of the target hemifield, but the target could appear anywhere along a 90° arc, also centered across the horizontal meridian, at 4.5° central eccentricity. For the 50% certainty condition, the two hemifields of the cue were either completely green or completely red, indicating that the upcoming target would appear anywhere along the 180° semicircle (a whole hemifield) at 4.5° central eccentricity. For the 0% certainty condition, no lines or wedges were

presented, indicating that the upcoming target would appear anywhere around the 360° circle at 4.5° central eccentricity. Cue condition (100%, 75%, 50%, or 0% cue certainty) and target hemifield were randomized on a trial-by-trial basis.

The visual target consisted of a plus sign enclosed by a circle. Participants were tasked to indicate, via manual button press with their dominant hand, whether the plus was exactly vertical and horizontal (index finger) or slightly rotated (middle finger). A non-target stimulus was simultaneously presented in the opposite hemifield, mirrored across the vertical meridian. This non-target stimulus was a box enclosed by a circle, its basic visual components (two horizontal and two vertical bars enclosed in a circle) thus similar to that of targets.

Prior to the main experiment, each participant underwent individual psychophysical thresholding to normalize accuracy across participants. The thresholding procedure was a two-down, one-up staircase converging on ~70% accuracy (Leek, 2001). In the thresholding task, participants were only presented with 50% certainty cues and were initially shown either a vertical “+” or a 45°-rotated “X”. With every correct trial, the “X” rotated 1.5° closer toward vertical, and with every incorrect response, it rotated 3.0° away from vertical. Once behavioral asymptote was reached, the average angle across the final 10 trials was used as the final angle for the main experiment.

Data Acquisition

EEG data was collected using a BioSemi ActiveTwo 64-channel DC amplifier with 24-bit resolution and was sampled at 1024 Hz. In addition to 64 scalp electrodes,

both horizontal (HEOG) and vertical (VEOG) electrooculograms were recorded at both external canthi and with a left-inferior eye electrode, respectively. Data was referenced offline to the average potential of two mastoid electrodes. To ensure exact timing relative to stimulus presentation, event onset times were based on timing information provided by a photodiode attached to the stimulus presentation monitor.

Data Processing

Data was preprocessed and analyzed in MATLAB® (R2017a, Natick, MA) and Python with custom scripts using the EEGLAB MATLAB toolbox (Delorme and Makeig, 2004), the CircStats MATLAB toolbox (Berens, 2009), and the FOOOF Python module (Haller and Donoghue et al., 2018). Continuous EEG data was resampled from 1024 Hz to 256 Hz. Data was highpass filtered above 1 Hz using a one-way, Hamming-windowed sinc finite impulse response (FIR) filter (-6 dB cutoff frequency 0.5 Hz, 1 Hz transition band) and lowpass filtered below 50 Hz using a one-way, Hamming-windowed sinc FIR filter (-6dB cutoff frequency 56.25 Hz, 12.5 Hz transition band). Bad channels (no more than 4 per participant) were spherically interpolated. Of those with interpolated channels, there was an average of 2.23 channels (3.5% of channels) per participant.

Baseline noise and response variability were assessed using pre-trial and target-evoked EEG activity, respectively. For baseline noise, epochs containing the 500 ms of activity prior to spatial cue onset were extracted (-500 to 0 ms relative to cue onset). Cue-locked epochs were rejected if the amplitude of any EEG channel exceeded ± 125 μV, any frontal EEG channel exceeded ± 75 μV, either HEOG channel exceeded ± 40 μV, or the difference between HEOG channels exceeded ± 40 μV. Response variability was assessed using the 1000 ms of activity centered around target onset (-500 to 500

ms relative to target onset). A similar epoch rejection procedure was used, though in the case of target-locked epochs, both pre-cue and pre-target baselines (-100 to 0 ms) were used to detect artifacts. Trials were rejected independently between cue- and target-locked epochs. Due to low trial numbers after artifact rejection, 6 and 9 younger and older adults, respectively, were excluded from further analysis for each having fewer than thirty total (irrespective of cue condition) clean target-locked epochs from correctly answered trials. For clean cue-locked epochs from correctly answered trials, there was no difference in total epoch number between younger and older adults (p = 0.27). For clean target-locked epochs from correctly answered trials, there was no difference in total epoch number between groups (p = 0.34), nor was there a difference in epoch number between groups in any cue condition (100%: p = 0.49; 75%: p = 0.56; 50%: p = 0.38; 0%: p = 0.11).

Data Analysis

Baseline noise was estimated using the exponent of the 1/*f*-like EEG power spectrum (Voytek et al., 2015; Gao et al., 2017). Specifically, each clean cue-locked epoch per channel was tapered with a Hanning window and zero-padded to one second in length. Using this zero-padded tapered trial, a power spectrum was constructed using the absolute value squared of the complex-numbered output of the Discrete Fourier Transform. This power spectrum was then decomposed using the FOOOF algorithm, which separates power spectra into aperiodic, 1/*f*-like components and zero or more oscillatory peaks whose power exceeds that of aperiodic activity by some threshold. With FOOOF, we extracted the aperiodic component over the 2-to-20-Hz frequency range of each power spectrum (*aperiodic_mode* = ‘fixed’, *peak_width_limits* = [2, inf],

peak_threshold = 1, and default settings otherwise). The negative of the corresponding aperiodic exponent was used as 1/*f* slope to index pre-cue baseline noise.

Response variability was quantified using trial-by-trial alpha phase consistency, or alpha intertrial phase coherence (ITC). To calculate ITC, clean target-locked epochs padded with an extra second of data per side were bandpass filtered with a one-way, Hamming-windowed sinc FIR filter (2 Hz transition band) with a 4 Hz passband centered on each participant's peak alpha frequency (PAF). Each participant's PAF was estimated using power spectra constructed using the activity of channel Oz during target-locked epochs (-500 to 500 ms) and as the average across trials of the frequency of maximum power between 7 and 14 Hz. This frequency was determined using oscillatory peaks extracted with FOOOF (*aperiodic_mode* = 'fixed', *peak_width_limits* = [2, inf], *peak_threshold* = 1, and default settings otherwise). Estimates of PAF did not differ between younger and older adults ($p = 0.18$), and across all participants, PAF estimates did not differ between usage of *peak_threshold* 1 and 2 ($p = 0.75$) or between *peak_threshold* 1 and 3 ($p = 0.79$). The angle of the Hilbert transform of the bandpass filtered data was used to extract alpha analytic phase. The phase time series consists of cosine phase values of (π, π] radians, with π radians corresponding to the trough and zero radians to the peak of the oscillation. This method yields results equivalent to sliding-window fast Fourier transform and wavelet approaches (Bruns, 2004). The mean vector length of each timepoint's phase distribution across trials was calculated. This mean vector length represents the degree of ITC, with ITC of unity reflecting a single adopted phase across trials and a value of zero reflecting uniformly distributed phases across trials.

Statistical Analyses

Correctly answered trials from all cue conditions were pooled together for EEG analyses. To normalize electrode locations, channel recordings were swapped right to left across the midline as though targets were always presented in the right visual hemifield, making left- and right-hemisphere channels contralateral and ipsilateral to all targets, respectively. All analyses were performed on data from EEG channels O1/2, PO3/4, and PO7/8, with channels O1, PO3, and PO7 considered contralateral to targets. For baseline noise estimates, 1/*f* slope values were averaged across contralateral and ipsilateral channels separately. For response variability estimates, and because of ITC values being sensitive to differences in the number of data points used, we implemented a random resampling procedure to control for differences in epoch number between participants. Per participant, we randomly selected 30 target-locked epochs without replacement, and using these epochs, we constructed ITC time series per channel of interest. These time series were baselined using the -500 to 0 ms window prior to target onset and averaged across contralateral and ipsilateral channels separately. Peak ITC in the 0 to 500 ms after target onset was then determined. This procedure was repeated 2000 times per participant, and the median of this distribution was used for subsequent statistical analysis.

Multiple-factor statistical analyses were assessed via ANOVAs, with age as a between-group factor and hemisphere as a within-group factor. Where sphericity assumptions were violated, degrees of freedom were adjusted using Greenhouse-Geisser corrections. Because ITC values prior to baselining are bound between 0 and 1, peak ITC values were $\log_{10}$-transformed prior to ANOVA analysis, and any single-

factor comparisons or correlations involving ITC were analyzed using non-parametric tests. Ultimately, 25 out of 31 younger adults and 20 out of 29 older adults were included in the final analysis. One older participant was excluded only from behavioral response time analyses due to a lack of correct trials in the 0% certainty condition.

Results

Older adults had lower accuracy and longer response times

We compared younger and older adults' accuracy levels in a visual discrimination task in which pre-target spatial cues had varying levels of information about the locations of upcoming targets (Figure 2.1A). Accuracy showed main effects of age and cue information as well as an interaction between the two (age: $F_{1,43} = 8.52$, $p = 0.0056$, $\eta^2 = 0.091$; cue: $F_{3,129} = 38.01$, $\varepsilon = 0.47$, $p_{GG} < 10^{-8}$, $\eta^2 = 0.30$; age*cue: $F_{3,129} = 8.14$, $\varepsilon = 0.47$, $p_{GG} = 0.0024$, $\eta^2 = 0.085$). Post-hoc analysis indicated that younger and older adults did not differ in accuracy in the 100% or 75% certainty conditions ($p = 0.36$; $p = 0.57$), but older adults trended towards showing modest accuracy deficits in the 50% condition ($p = 0.071$) and had significant deficits in the 0% condition (Figure 2.1B; 74% vs 52%, $t_{21.48} = 3.48$, $p = 0.0022$, Cohen's $d = 1.15$).

We also examined differences in response time between younger and older adults. As with accuracy, response time showed an interaction between age and cue information in addition to separate main effects of each (age: $F_{1,42} = 36.60$, $p < 10^{-6}$, $\eta^2 = 0.41$; cue: $F_{3,126} = 68.09$, $\varepsilon = 0.43$, $p_{GG} < 10^{-17}$, $\eta^2 = 0.23$, age*cue: $F_{3,126} = 3.52$, $\varepsilon = 0.43$, $p_{GG} = 0.035$, $\eta^2 = 0.016$). Post-hoc analysis indicated that older adults had longer response times in all cue conditions (Figure 2.1C; 100%: 584 ms vs. 728 ms, $t_{41.04} =$ -

5.78, $p < 10^{-6}$, Cohen's d = -1.73; 75%: 643 ms vs. 779 ms, $t_{40.26}$ = -4.64, $p < 10^{-4}$, Cohen's d = -1.40; 50%: 664 ms vs. 817 ms, $t_{41.09}$ = -5.40, $p < 10^{-5}$, Cohen's d = -1.61; 0%: 703 ms vs. 900 ms, $t_{37.78}$ = -6.17, $p < 10^{-6}$, Cohen's d = -1.89).

Figure 2.1. Spatial attention task and behavioral performance results. (A) Trial structure and visual stimuli presented. Cues presented at the beginning of each trial contained varying levels of spatial information about upcoming targets (plus signs enclosed in circles), indicating with green wedges of varying sizes the hemifield and potential location of targets. Targets were always presented at 4.5^{o} central eccentricity and simultaneously presented with non-target stimuli of matched visual properties in the opposite visual hemifield, mirrored across the meridian. In the 100% certainty condition, targets appeared exactly to the left or right of center. In the 75% certainty condition, targets appeared anywhere in a 90^{o} arc in the indicated hemifield. In the 50% certainty condition, targets appeared anywhere in a 180^{o} arc in the indicated hemifield. In the 0% certainty condition, green wedges were not supplied, and targets appeared anywhere in the full 4.5^{o} central eccentricity circle. Potential target locations are indicated here with green arcs (not actually shown to participants). (B) Younger (blue) and older (green) adults' accuracy across cue conditions (participants plotted individually, error bars of standard deviation). Older adults had lower accuracy than younger adults only in the 0% certainty condition (** $p < 0.01$). (C) Younger (blue) and older (green) adults' response times across cue conditions (participants plotted individually, error bars of standard deviation). Older adults had slower response times than younger adults in all cue conditions (*** $p < 0.001$ for each).

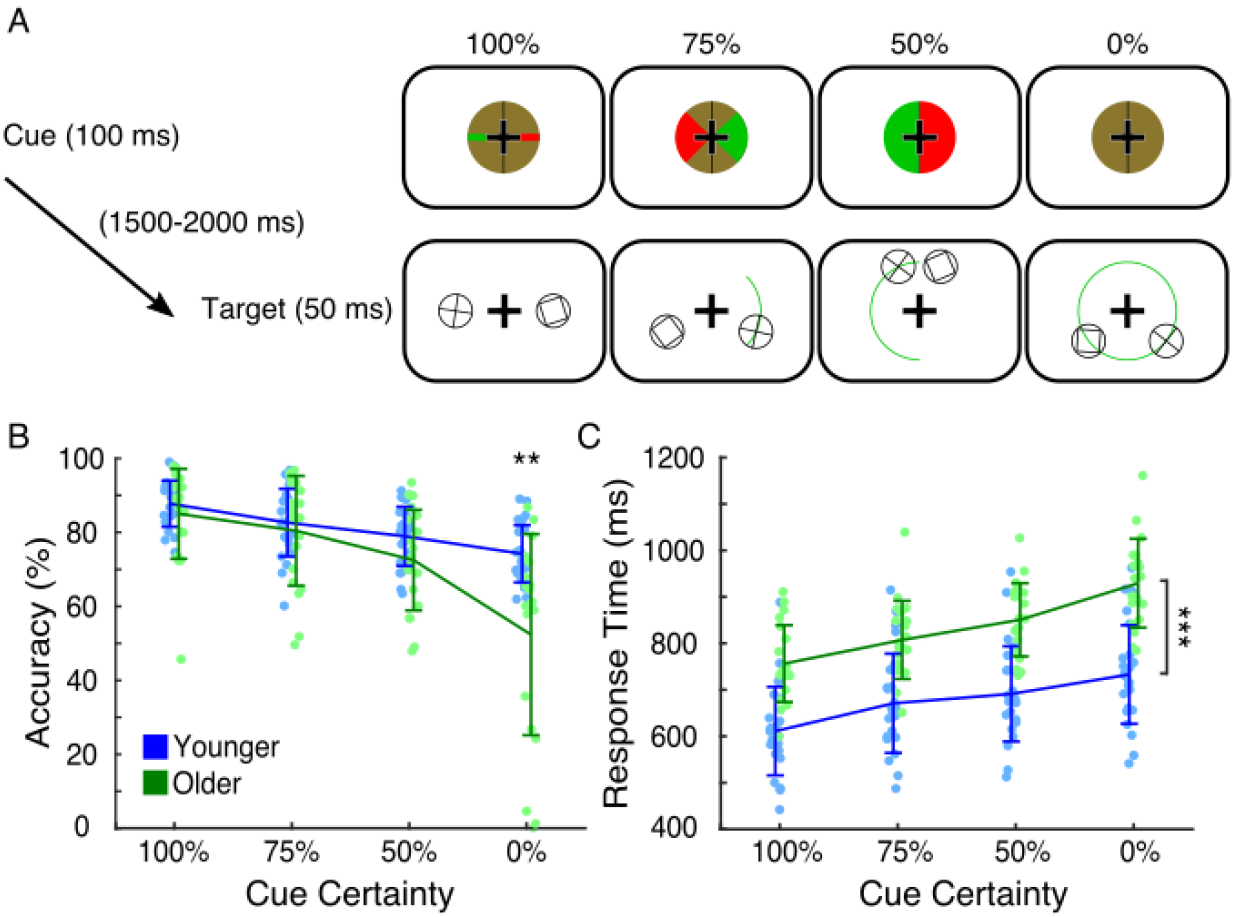
A
100%
75%
50%
0%
Cue (100 ms)
(1500-2000 ms)
Target (50 ms)
B
Accuracy (%)
100
80
60
40
20
0
**
Younger
Older
100%
75%
50%
0%
Cue Certainty
C
Response Time (ms)
1200
1000
800
600
400
***
100%
75%
50%
0%
Cue Certainty

Baseline noise and response variability were elevated in older adults

We estimated pre-trial baseline noise levels using the 1/*f*-like power spectrum slope of pre-cue visual posterior EEG activity. To do so, we pooled trials from all cue conditions and examined average 1/*f* slope contralateral and ipsilateral to attended target locations. Baseline 1/*f* slope showed a main effect of age (Figure 2.2; age: -1.03 vs. -0.81, $F_{1,43} = 12.54$, $p < 10^{-3}$, $\eta^2 = 0.22$), but no main effect of hemisphere or interaction between age and hemisphere (hemisphere: $F_{1,43} < 1.0$, $p = 0.42$; age*hemisphere: $F_{1,43} = 3.35$, $p = 0.074$). These results indicate that older adults had higher levels of pre-trial baseline noise than did younger adults.

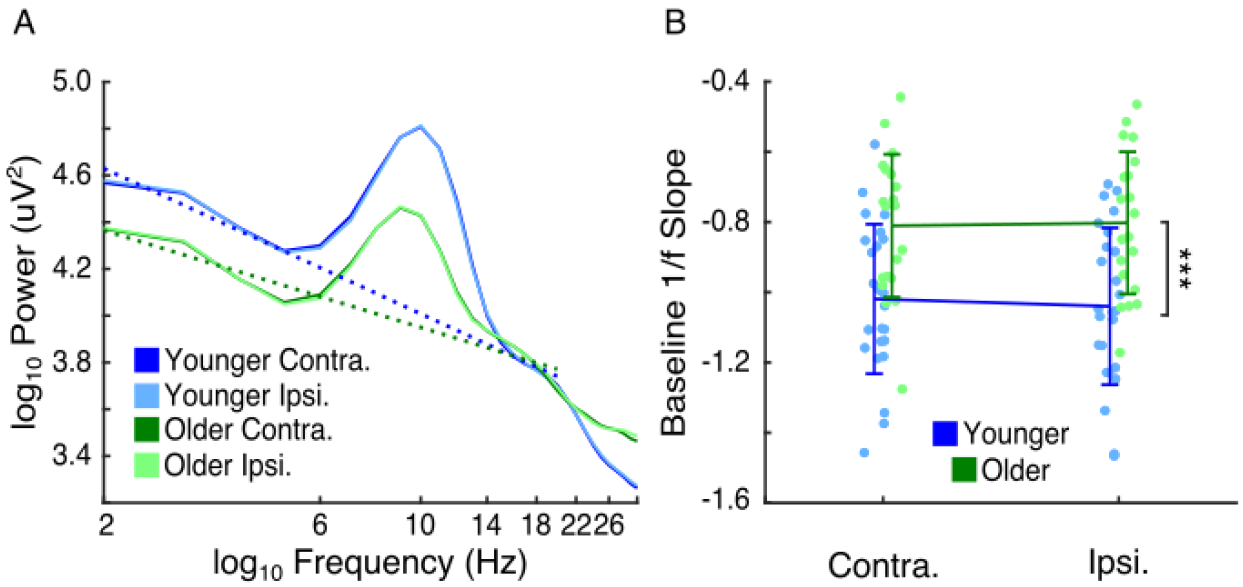

Figure 2.2. Baseline noise, characterized using the 1/*f*-like power spectrum slope of pre-trial visual EEG activity, was higher in older adults. (A) Grand-average log-log-space power spectra of younger (blue) and older adults (green) both contralateral (darker) and ipsilateral (lighter) to eventual target presentation. Dotted lines indicate estimated 1/*f* slopes. (B) Contralateral and ipsilateral 1/*f* slope values of younger (blue) and older (green) adults (participants plotted individually, error bars of standard deviation). Older adults had higher 1/*f* slope values (main effect of age, ***$p < 0.001$), suggesting higher levels of pre-trial baseline noise.

To estimate trial-by-trial response variability, we calculated the intertrial phase coherence (ITC) of target-evoked alpha-band phase responses (Figure 2.3A). Peak ITC after target onset showed a main effect of age, with older adults having lower evoked ITC than younger adults (Figure 2.3B; 0.29 vs 0.23, $F_{1,43} = 4.11$, $p = 0.049$, $\eta^2 = 0.079$). There was no main effect of hemisphere or interaction between age and hemisphere (hemisphere: $F_{1,43} < 1.0$, $p = 0.52$; age*hemisphere: $F_{1,43} < 1.0$, $p = 0.36$). Thus, older adults had higher variability in their target-evoked alpha phase responses than did younger adults.

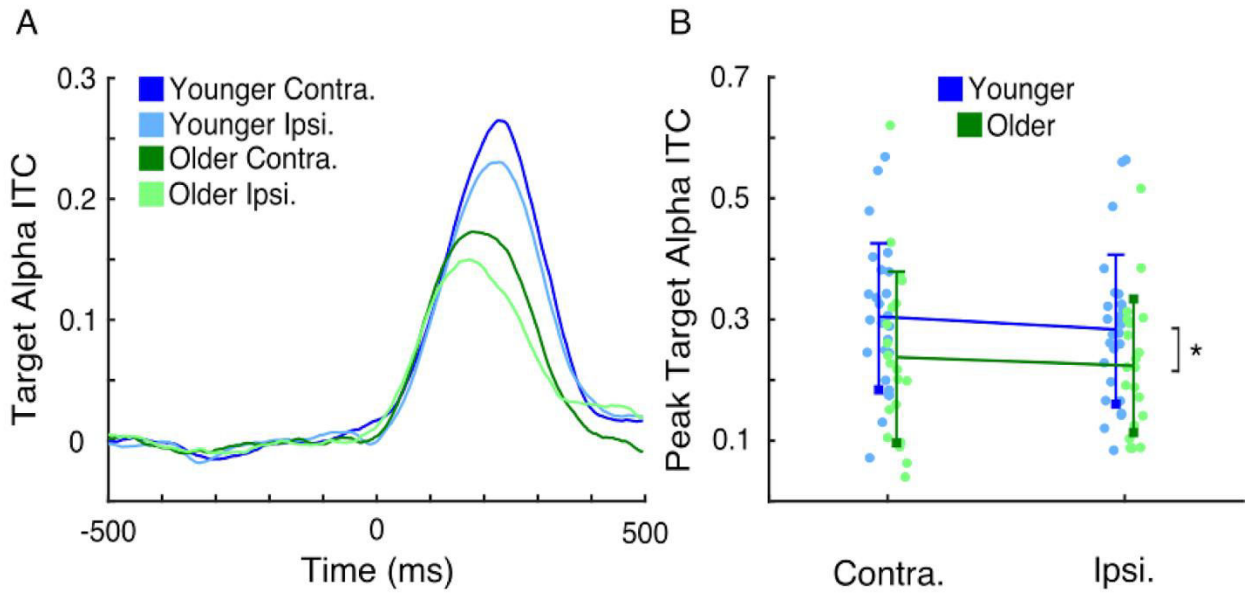

Figure 2.3. Trial-by-trial response variability, characterized using the consistency of target-evoked alpha phase responses (alpha intertrial coherence, or ITC), was elevated in older adults. (A) Grand-average time courses of baselined target-evoked alpha ITC of younger (blue) and older adults (green) both contralateral (darker) and ipsilateral (lighter) to target presentation. (B) Contralateral and ipsilateral peak alpha ITC values of younger (blue) and older (green) adults (participants plotted individually, error bars of standard deviation). Older adults had lower peak alpha ITC values (main effect of age, $*p < 0.05$), indicating higher levels of response variability.

Baseline noise was correlated with response variability in older adults

Given the observed age-related differences in baseline noise and response variability, we next investigated the relationship between these two measures. Specifically, we examined if, within groups, higher levels of baseline noise would be associated with increased variability in target-evoked alpha phase responses. In younger adults, no relationship between 1/*f* slope and peak alpha ITC was observed contralateral or ipsilateral to target presentation (Figure 2.4A; $p = 0.88$, $p = 0.72$). In older adults, on the other hand, participants with flatter 1/*f* slopes also had lower levels of evoked alpha ITC, and this was the case both contralateral (Figure 2.4B; Spearman's $r = -0.45$, $p = 0.047$) and ipsilateral to target presentation (Spearman's $r = -0.57$, $p = 0.0094$). The correlation between 1/*f* slope and evoked alpha ITC was stronger for older versus younger adults ipsilaterally (Fisher's *z*-transform = 1.78, $p = 0.037$) and trended similarly contralaterally (Fisher's *z*-transform = 1.60, $p = 0.055$). Thus, older but not younger participants with more baseline noise also had higher variability in stimulus-evoked responses.

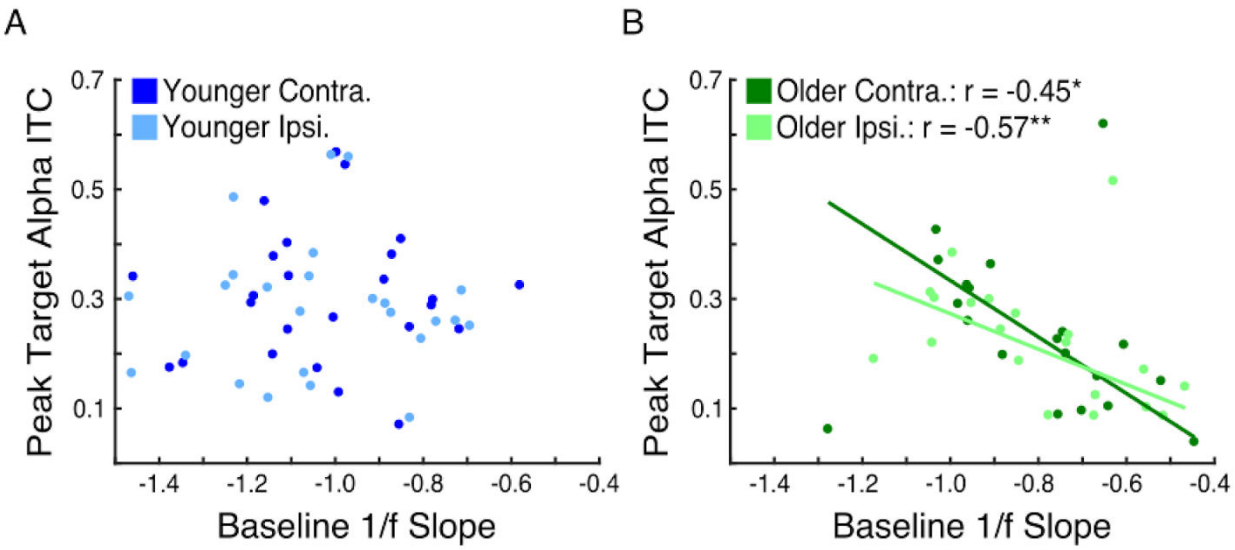

Figure 2.4. Baseline noise and response variability were correlated in older but not younger adults. (A) Peak target-evoked alpha ITC versus baseline 1/*f* slope in younger adults both contralateral (darker) and ipsilateral (lighter) to target presentation. No relationship was found. (B) Peak target-evoked alpha ITC versus baseline 1/*f* slope in older adults, with best-fit lines both contralateral (darker) and ipsilateral (lighter) to target presentation. In both hemispheres, increased baseline noise (less negative or flatter pre-trial 1/*f* slope) was associated with increased response variability (reduced peak target-evoked alpha ITC, *$p < 0.05$, **$p < 0.01$).

Trial-by-trial response variability was correlated with accuracy in younger adults

We also examined whether levels of baseline noise or response variability were related to behavioral performance. For this investigation, accuracy across all trials (irrespective of cue condition) was used. Baseline 1/*f* slope contralateral to target presentation was not correlated with accuracy in younger or older adults (Figure 2.5A; Younger: $p = 0.62$; Older: $p = 0.34$). Regarding response variability, however, higher target-evoked contralateral alpha ITC was correlated with higher accuracy in younger adults (Figure 2.5B; Spearman's $r = 0.51$, $p = 0.0096$). No such relationship was found across older adults ($p = 0.51$). Thus, contralateral alpha phase response consistency was related to behavioral performance in younger adults, though not in older adults.

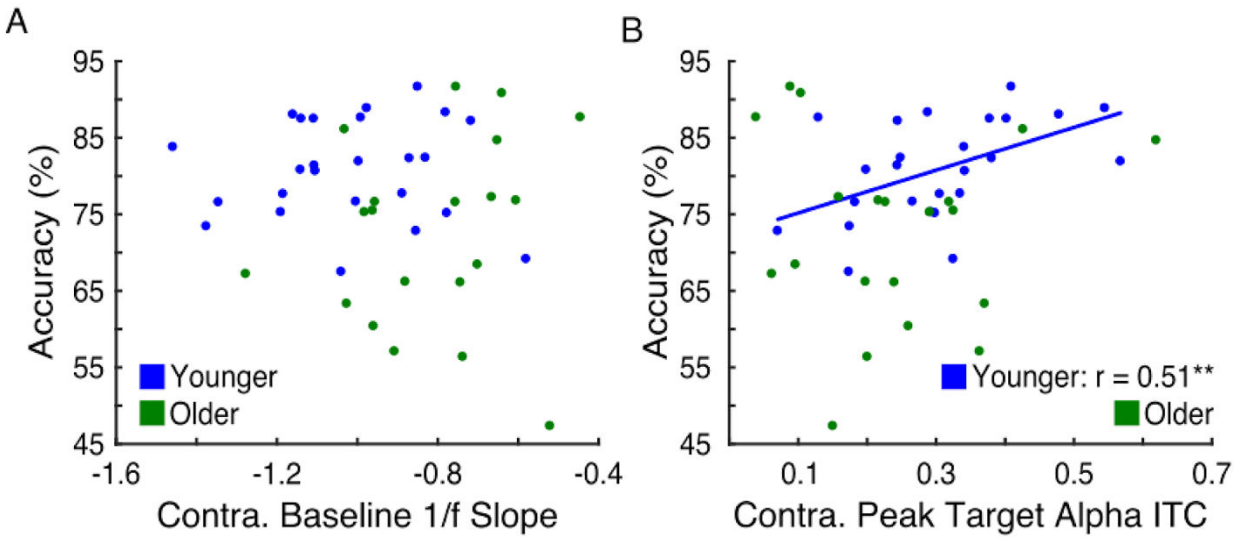

Figure 2.5. Baseline noise was not correlated with behavioral accuracy, but decreased response variability was associated with higher accuracy in younger but not older adults. (A) Accuracy across all cue conditions versus contralateral baseline 1/*f* slope in younger (blue) and older (green) adults. No relationship was found. (B) Accuracy versus contralateral peak target-evoked alpha ITC in younger (blue) and older (green) adults, with best-fit line for younger adults. In younger but not older adults, higher alpha ITC was associated with higher accuracy (**$p < 0.01$).

Discussion

In this study, we sought to examine the relationship between two types of neural noise—tonic baseline noise and trial-by-trial response variability—as well as how age-related changes in either relate to cognitive decline. We compared younger and older adults' behavioral performance and visual cortical activity during a spatial visual discrimination task. Analysis of visual posterior EEG activity demonstrated that pre-trial baseline noise, characterized using 1/*f* slope, was elevated in older adults relative to younger adults. In addition, we found that older adults also had greater inconsistency in their alpha phase responses to target presentation. In younger adults, alpha phase response consistency was correlated with higher accuracy, though not so in older adults. In older—but not younger—adults, higher baseline noise was associated with greater target-evoked response variability.

Concerning behavioral performance, older adults had longer response times relative to younger adults in each cue condition, but lower accuracy only when no spatial information was provided about upcoming targets. Comparable accuracy in task conditions where spatial information was provided indicates that both groups were using provided cue information to guide behavior. In the absence of spatial information, however, the briefness of target presentation and any difficulty in quickly distinguishing targets from non-targets (as in the 0% certainty condition, participants were unaware of the visual hemifield in which targets would eventually appear) may have contributed to lower accuracy in older adults.

As has been found in previous studies, pre-trial 1/*f* slope was flatter in older adults (Voytek et al., 2015; Waschke et al., 2017; McNair et al., 2018). More broadly,

the 1/*f* slope of neural activity has been studied in the context of neural population spiking statistics (Voytek et al., 2015; Voytek and Knight, 2015; Gao, 2015), excitatory-inhibitory (EI) balance (Gao et al., 2017), cortical activation (Podvalny et al., 2015), and neural irregularity (Waschke et al., 2017). That 1/*f* slope is flatter in older adults is thus consistent with previous findings of age-related increases in spontaneous, asynchronous baseline activity (Hong and Rebec, 2012) and could be indicative of age-related shifts in EI balance (Gao et al., 2017) and reductions in inhibitory signaling (Hickmott and Dinse, 2013).

Additionally, target-evoked alpha ITC was elevated in younger adults and correlated with behavioral performance in younger but not older adults. This relationship between target-evoked alpha phase response consistency and behavioral performance is consistent with previous findings (Klimesch et al., 2004; Hanslmayr et al., 2005; Werkle-Bergner et al., 2012; Yamagishi et al., 2008; Tran et al., 2016) and indicates that the degree to which cortical neural populations can precisely respond to external stimuli directly influences behavioral outcomes in younger adults. Age-related reductions in stimulus-evoked alpha phase consistency, as reported here and previously (Tran et al., 2016), suggest that such precision in sensory processing is reduced in older adults. At the same time, the lack of correlation between target-evoked alpha phase response consistency and accuracy across older adults in this study also suggests that later processes are themselves altered as to account or compensate for these changes in early sensory processing.

Other studies, however, have reported no difference (Werkle-Bergner et al., 2012) or even elevated stimulus-evoked alpha ITC in older adults (Sander et al., 2012;

Wiegand and Sander, 2019). These reported increases in alpha ITC are hypothesized to reflect older adults' excessive neural entrainment to external stimuli, with such entrainment impeding subsequent processes necessary for successful behavioral outcomes. Contradictory results between these studies and the present study could be, and are likely due to, differences in the properties of stimuli being presented. For instance, here and in Tran et al., 2016, age-related changes in stimulus-evoked alpha phase responses were investigated for visual stimuli presented for only 50 ms durations. As such, these visual stimuli could have been insufficient to entrain older adults in the manner demonstrated in Sander et al., 2012, and Wiegand and Sander, 2019, which examined the alpha phase responses to visual stimuli of 100 ms duration and 85 dB tones, respectively. Moreover, that visual targets in this study were only 50 ms in duration, such duration being less than one alpha oscillation cycle in length, suggests that target presentation sometimes fell partially or even entirely during alpha phases non-optimal for sensory processing (Busch and VanRullen, 2010; Mathewson et al., 2009). If alpha phase effects are more pronounced in older adults–for instance, if older adults have larger differences in perceptual processing between optimal and non-optimal alpha phases–these changes could lead to more variable evoked responses to briefly presented stimuli. This might account for the inconsistency in target-evoked alpha phase responses we observed here in older adults.

As hypothesized, pre-trial 1/*f* slope was correlated with target-evoked alpha ITC in older adults, with flatter 1/*f* slope associated with reduced alpha phase response consistency. This result suggests that age-related changes in neural activity, such changes apparent even in the absence of external stimuli, might hamper older adults'

ability to consistently respond to and process upcoming stimuli. This might occur due to a shift towards a more excitatory state (Gao et al., 2017) wherein increased asynchrony in or rate of spiking activity (Voytek et al., 2015; Voytek & Knight, 2015) might reduce the consistency of visual stimulus processing. In addition, increased age-related noise in ongoing neural activity, if such noise persists through and after stimulus presentation, could dominate relatively weak or inconsistent responses to short-duration stimuli. Interestingly, a relationship between pre-trial 1/*f* slope and target-evoked alpha ITC was not present in younger adults. These results suggest that at the levels of baseline noise shown in younger adults, phase response consistency is largely unaffected by individual differences in ongoing baseline noise. In older adults, on the other hand, elevations in baseline noise levels might point to profound changes in ongoing neural activity that, if more greatly exacerbated, lead to greater effects on subsequent sensory processing.

Conclusion

Overall, we find that baseline noise and stimulus-evoked trial-by-trial response variability are both elevated during healthy aging, with increases in baseline noise associated with increased alpha phase response variability across older adults. Thus, age-related changes in sensory processing may be due in part to alterations in neural population activity that can be observed in ongoing, non-stimulus-evoked activity. These alterations may include age-related increases in neural asynchrony or EI balance, with such increases potentially affecting the capacity of older adults to reliably respond to upcoming stimuli. These findings point to the need for greater understanding of the

ways in which age-related changes in ongoing neural activity or neural noise in general might affect neural mechanisms supporting sensory processing and cognition.

Chapter 2, in full, has been submitted for publication of the material. Tran, T. T., Rolle, C. E., Gazzaley, A. & Voytek, B. Linked sources of neural noise contribute to age-related cognitive decline. The dissertation author was the primary investigator and author of this paper.

References

Berens, P., 2009. CircStat: A MATLABToolbox for Circular Statistics. J. Stat. Soft. 31, 1–21.

Bruns, A., 2004. Fourier-, Hilbert- and wavelet-based signal analysis: are they really different approaches? Journal of Neuroscience Methods 137, 321–332.

Busch, N.A., Dubois, J., VanRullen, R., 2009. The phase of ongoing EEG oscillations predicts visual perception. J. Neurosci. 29, 7869–7876.

Cremer, R., Zeef, E.J., 1987. What Kind of Noise Increases With Age? Journal of Gerontology 42, 515–518.

Delorme, A., Makeig, S., 2004. EEGLAB: an open source toolbox for analysis of single-trial EEG dynamics including independent component analysis. Journal of Neuroscience Methods 134, 9–21.

Dinstein, I., Heeger, D.J., Behrmann, M., 2015. Neural variability: friend or foe? Trends in Cognitive Sciences 19, 322–328.

Faisal, A.A., Selen, L.P.J., Wolpert, D.M., 2008. Noise in the nervous system. Nat Rev Neurosci 9, 292–303.

Gao, R., 2016. Interpreting the electrophysiological power spectrum. Journal of Neurophysiology 115, 628–630.

Gao, R., Peterson, E.J., Voytek, B., 2017. Inferring synaptic excitation/inhibition balance from field potentials. NeuroImage 158, 70–78.

Haller, M., Donoghue, T., Peterson, E., Varma, P., Sebastian, P., Gao, R., Noto, T., Knight, R.T., Shestyuk, A., Voytek, B., 2018. Parameterizing neural power spectra. bioRxiv 299859.

Hanslmayr, S., Klimesch, W., Sauseng, P., Gruber, W., Doppelmayr, M., Freunberger, R., Pecherstorfer, T., 2005. Visual discrimination performance is related to decreased alpha amplitude but increased phase locking. Neuroscience Letters 375, 64–68.

He, B.J., 2014. Scale-free brain activity: past, present, and future. Trends in Cognitive Sciences 18, 480–487.

Hickmott, P., Dinse, H., 2013. Effects of Aging on Properties of the Local Circuit in Rat Primary Somatosensory Cortex (S1) In Vitro. Cerebral Cortex 23, 2500–2513.

Hong, S.L., Rebec, G.V., 2012. A new perspective on behavioral inconsistency and neural noise in aging: compensatory speeding of neural communication. Frontiers in Aging Neuroscience 4, 1–6.

Klimesch, W., Schack, B., Schabus, M., Doppelmayr, M., Gruber, W., Sauseng, P., 2004. Phase-locked alpha and theta oscillations generate the P1–N1 complex and are related to memory performance. Cognitive Brain Research 19, 302–316.

Kügler, C.F., Taghavy, A., Platt, D., 1993. The event-related P300 potential analysis of cognitive human brain aging: a review. Gerontology 39, 280–303.

Leek, M.R., 2001. Adaptive procedures in psychophysical research. Percept Psychophys 63, 1279–1292.

Lorenzo-López, L., Amenedo, E., Pazo-Álvarez, P., Cadaveira, F., 2007. Visual target processing in high- and low-performing older subjects indexed by P3 component. Neurophysiologie Clinique/Clinical Neurophysiology 37, 53–61.

Mathewson, K.E., Gratton, G., Fabiani, M., Beck, D.M., Ro, T., 2009. To See or Not to See: Prestimulus Alpha Phase Predicts Visual Awareness. Journal of Neuroscience 29, 2725–2732.

McNair, S.W., Kayser, S.J., Kayser, C., 2019. Consistent pre-stimulus influences on auditory perception across the lifespan. NeuroImage 186, 22–32.

Miller, K.J., Sorensen, L.B., Ojemann, J.G., Nijs, den, M., 2009. Power-Law Scaling in the Brain Surface Electric Potential. PLoS Comput Biol 5, e1000609.

Podvalny, E., Noy, N., Harel, M., Bickel, S., Chechik, G., Schroeder, C.E., Mehta, A.D., Tsodyks, M., Malach, R., 2015. A unifying principle underlying the extracellular field potential spectral responses in the human cortex. Journal of Neurophysiology 114, 505–519.

Rolle, C.E., Anguera, J.A., Skinner, S.N., Voytek, B., Gazzaley, A., 2017. Enhancing Spatial Attention and Working Memory in Younger and Older Adults. Journal of Cognitive Neuroscience 29, 1483–1497.

Rolle, C.E., Voytek, B., Gazzaley, A., 2015. Exploring the Potential of the iPad and Xbox Kinect for Cognitive Science Research. Games for Health Journal 4, 221–224.

Sander, M.C., Werkle-Bergner, M., Lindenberger, U., 2012. Amplitude modulations and inter-trial phase stability of alpha-oscillations differentially reflect working memory constraints across the lifespan. NeuroImage 59, 646–654.

Scholvinck, M.L., Saleem, A.B., Benucci, A., Harris, K.D., Carandini, M., 2015. Cortical State Determines Global Variability and Correlations in Visual Cortex. Journal of Neuroscience 35, 170–178.

Tran, T.T., Hoffner, N.C., LaHue, S.C., Tseng, L., Voytek, B., 2016. Alpha phase dynamics predict age-related visual working memory decline. NeuroImage 143, 196–203.

Voytek, B., Knight, R.T., 2015. Dynamic Network Communication as a Unifying Neural Basis for Cognition, Development, Aging, and Disease. Biological Psychiatry 77, 1089–1097.

Voytek, B., Kramer, M.A., Case, J., Lepage, K.Q., Tempesta, Z.R., Knight, R.T., Gazzaley, A., 2015. Age-Related Changes in 1/f Neural Electrophysiological Noise. Journal of Neuroscience 35, 13257–13265.

Voytek, B., Samaha, J., Rolle, C.E., Greenberg, Z., Gill, N., Porat, S., Kader, T., Rahman, S., Malzyner, R., Gazzaley, A., 2017. Preparatory Encoding of the Fine Scale of Human Spatial Attention. Journal of Cognitive Neuroscience 29, 1302–1310.

Waschke, L., Tune, S., Obleser, J., 2019. Neural desynchronization and arousal differentially shape brain states for optimal sensory performance. bioRxiv 582353.

Waschke, L., Wöstmann, M., Obleser, J., 2017. States and traits of neural irregularity in the age-varying human brain. Scientific Reports 7, 17381.

Werkle-Bergner, M., Freunberger, R., Sander, M.C., Lindenberger, U., Klimesch, W., 2012. Inter-individual performance differences in younger and older adults differentially relate to amplitude modulations and phase stability of oscillations controlling working memory contents. NeuroImage 60, 71–82.

Wiegand, I., Sander, M.C., 2019. Cue-related processing accounts for age differences in phasic alerting. Neurobiology of Aging 79, 93–100.

Yamagishi, N., Callan, D.E., Anderson, S.J., Kawato, M., 2008. Attentional changes in pre-stimulus oscillatory activity within early visual cortex are predictive of human visual performance. Brain Research 1197, 115–122.

CHAPTER 3: Frontal cortical aperiodic activity tracks successful memory encoding

Abstract

Successful memory encoding is associated with dynamic changes in temporofrontal cortical activity. Such changes include concomitant decreased and increased power in lower- and higher-frequency neural activity, respectively. However, it is unclear to what extent these changes might be due to differences in oscillatory activity (for instance, the amplitude of 4-8 Hz theta oscillations), aperiodic activity, or both. In this study, we investigated the differences specifically in aperiodic activity between episodes of successful and unsuccessful memory encoding. We also examined whether changes in aperiodic activity might also track, over time, the contents of short-term memory as more and more items are maintained. To do so, we analyzed previously collected electrocorticographic (ECoG) recordings from 28 patients who performed a delayed free recall task. In this task, patients were asked to memorize lists of serially, visually presented words. From these recordings, we assessed lateral temporal (LTL) and lateral frontal cortical (LFC) aperiodic activity using both the 1/*f*-like slope of the electrophysiological power spectrum as well as the amplitude of 80-150 Hz high-frequency activity (HFA). We found that LFC aperiodic slope was higher (flatter) prior to the presentation of subsequently recalled versus non-recalled words, and during word presentation itself, LFC HFA was higher for subsequently recalled versus non-recalled words as well. No such findings were observed for theta-HFA phase-amplitude coupling (PAC), either when examining all available electrodes or when examining only electrodes displaying prominent theta oscillations. We also found that while LFC aperiodic slope prior to word presentation on average decreased from the beginning to

end of lists, such pre-stimulus LFC aperiodic slope increased from the beginning to end of lists in which more words were subsequently recalled. These results suggest that successful memory encoding as well as the number of items maintained in short-term memory can be tracked using characteristics of LFC aperiodic activity. They also suggest that the degree to which frontal cortical neural populations can shift towards more asynchronous activity states has a direct effect on memory maintenance and capacity.

Introduction

Successful memory encoding is associated with widespread changes in neural activity. Power in lower frequencies, for instance in the 4-8 Hz theta band, is lower during the presentation of successfully versus unsuccessfully encoded memory items, while power in higher frequencies (> 30 Hz) is concomitantly higher (Burke et al., 2013). Such differences have been observed in a number of brain regions, including the lateral temporal lobe (LTL) and the lateral frontal cortex (LFC), and these observations have successfully been used to guide targeted electrical stimulation and rescue memory encoding (Ezzyat et al., 2018).

However, it remains unclear to what extent such observations are due to changes in oscillatory activity, aperiodic activity, or both. For instance, decreased power in the 4-8 Hz frequency band might reflect an amplitude reduction in ongoing or evoked theta oscillations, but it might also reflect a change in the 1/*f*-like, aperiodic slope of the electrophysiological power spectrum (Voytek et al., 2015; Haller et al., 2018). An increase or flattening of aperiodic slope in response to visual stimulus presentation has

previously been reported, such flattening synonymous with concomitant decreases and increases in lower- and higher-frequency activity, respectively (Podvalny et al., 2015). Changes in population-level spiking also lead to power changes at both lower and higher frequencies, especially so for 80-150 Hz high-frequency activity or HFA (Manning et al., 2009; Miller et al., 2012).

Additionally, the phase of theta oscillations has been shown to modulate HFA amplitude (Canolty et al., 2006; Tort et al., 2009; Voytek et al., 2010; Maris et al., 2011; van der Meij et al., 2012). This modulation, or theta-HFA phase-amplitude coupling (PAC), has been proposed to facilitate memory encoding through the precise coordination of spiking activity (Fries, 2005). Hippocampal theta-HFA PAC has previously been shown in humans to increase with memory load (Axmacher et al., 2010) and during successful memory encoding (Lega et al., 2015), but similar findings for cortical theta-HFA PAC are less apparent (Lega et al., 2015). It is possible that restricting the examination of theta-HFA PAC only to cortical recording sites in which prominent theta oscillations are observed would help resolve the role of cortical theta-HFA PAC in successful memory encoding. Specifically, cortical theta-HFA PAC could be assessed only at recording sites for which the power spectrum of neural activity displays a peak in the 4-8 Hz frequency band whose power sufficiently exceeds that of the surrounding frequencies (Haller et al., 2018).

Here, we investigate the differences in LTL and LFC aperiodic slope, HFA, and theta-HFA PAC between episodes of successful and unsuccessful memory encoding. To do so, we analyzed previously collected electrocorticographic (ECoG) recordings from 28 patients who performed a delayed free recall task. In this task, patients were

asked to memorize lists of visually, serially presented words (Burke et al., 2013; Solomon et al., 2017; Ezzyat et al., 2018). From these recordings, we measured LTL and LFC aperiodic slope, HFA, and theta-HFA PAC before and after each word presentation. We hypothesized that each measure would be higher during the presentation of subsequently recalled versus non-recalled words. We also examined to what extent changes in aperiodic slope or HFA from the beginning to end of a list might track the percentage of words subsequently recalled from that list. Finally, we examined across patients the relationships among aperiodic slope, HFA, and theta-HFA PAC as well as whether these measures were related to patient age or overall behavioral performance.

Materials and Methods

Subjects

Previously collected electrocorticographic (ECoG) and stereotactic electroencephalographic (sEEG) recordings from patients with medication-resistant epilepsy were analyzed for this study. These recordings were made available through the University of Pennsylvania Restoring Active Memory (RAM) Public Data Release dated September 30, 2016. In addition to the recordings themselves, this data release also provided demographic information, electrode atlas locations and coordinates, cortical surface renderings, seizure onset zone information, and behavioral data and session notes for each patient.

Behavioral Task

Only patients that performed the verbal delayed free recall task previously described (Burke et al., 2013; Solomon et al., 2017; Ezzyat et al., 2018) were selected for subsequent pre-processing (the FR1 task in the RAM Public Data Release). In this task, a computer screen was used to present lists of 12 common nouns, and patients were instructed to study and memorize as many words as possible. For each list, words were presented sequentially and in capital letters at the center of the screen for 1600 ms, and each word was followed by a blank interstimulus interval varying in length between 750 and 1000 ms. At the end of each list, a 20-second distractor task was administered. In the distractor task, patients were asked to solve a series of arithmetic problems in which patients provided the sum of three randomly chosen integers ranging from 1 to 9. At the end of the distractor task, patients were given 30 seconds to verbally recall in any order as many words as possible from the preceding list.

Electrophysiological Recordings

As previously described (Burke et al., 2013; Solomon et al., 2017; Ezzyat et al., 2018), ECoG and sEEG data were collected from surgically implanted subdural grid, strip, and depth recording electrodes. Depending on hospital equipment and procedures, recordings were sampled anywhere between 256 and 1024 Hz and referenced to a common contact placed either intracranially or on the scalp or mastoid process. Electrodes were localized by co-registering postoperative computed tomographies (CTs)with postoperative MRIs when possible and with preoperative MRIs otherwise.

Pre-Processing

Of patients performing the free recall task, only patients that had at least three grid or strip (ECoG) electrodes in each of the lateral temporal lobe (LTL) and the lateral frontal cortex (LFC) were selected for subsequent pre-processing. LTL and LFC localization were determined using provided electrode location annotations. Of these 43 patients, one patient with unknown age, one patient with low recall performance (having less than 20 successfully recalled words), and one patient who did not perform the distractor task after each list were excluded.

For the remaining 40 patients, recordings were visually inspected for noise and epileptic activity. Electrodes whose recordings were excessively contaminated by noise were removed. Remaining electrode recordings were bandstop filtered using two-way, second-order Butterworth filters of sufficient bandwidth at any frequency between 50 and 250 Hz containing line noise.

All electrodes located in the seizure onset zone of the patient were removed. For further epileptic activity rejection, recordings were epoched into trials time-locked to word presentation (-1000 to 2750 ms relative to word presentation), and each trial was visually inspected. Any remaining electrodes whose recordings contained any epileptic activity, including interepileptic discharges, were removed from further analysis. In addition, trials during which any epileptic activity occurred, including interepileptic discharges and including in already removed electrodes, were excluded from further analysis (Parvizi and Kastner, 2018).

If such artifact rejection led to less than 20 remaining trials from subsequently recalled words or to less than three remaining ECoG electrodes in either the LTL or

LFC, the patient was excluded from further analysis. Out of 40 patients pre-processed in this manner, 12 patients were excluded, leaving 28 patients (17 female, 11 male) for further analysis. These patients had a median of 8 remaining ECoG electrodes in the LTL (minimum 3, maximum 32) and a median of 15.5 remaining ECoG electrodes in the LFC (minimum 3, maximum 41). On average, a median of 46.2% of ECoG electrodes were rejected in the LTL (minimum 0%, maximum 88.2%), and a median of 8.3% of ECoG electrodes were rejected in the LFC (minimum 0%, maximum 88.0%). Remaining ECoG electrodes were re-referenced to the common average reference. Only ECoG electrodes were included in subsequent analyses.

Remaining patients had on average a median of 277.5 total remaining trials (minimum 80, maximum 844) and a median of 66 remaining trials from subsequently recalled words (minimum 30, maximum 286). Remaining trials corresponded to a median of 25 lists per patient (minimum 15, maximum 85). A median of 22.2% of total trials were rejected (minimum 4.2%, maximum 72.5%).

Data Analysis

Time Windows of Interest

Neural activity features of interest were calculated for a pre-encoding time window from -750 to 0 ms relative to word presentation. Neural activity features of interest were also calculated for a late-encoding time window 800 to 1600 ms relative to word presentation.

Aperiodic Slope

Data was lowpass filtered below 200 Hz using a one-way, Hamming-windowed sinc finite impulse response (FIR) filter using default filter order and transition width settings from the FieldTrip software toolbox (Oostenveld et al., 2011). Separate power spectra per trial and electrode were constructed using pre- and late-encoding activity. Specifically, each time window per trial and electrode was tapered with a Hanning window, and power spectra were constructed using the absolute value squared of the complex-numbered output of the Discrete Fourier Transform. Power spectra were then decomposed using the FOOOF algorithm, which separates power spectra into aperiodic, 1/*f*-like components and zero or more oscillatory peaks whose power exceeds that of aperiodic activity by some threshold (Haller et al., 2018). With FOOOF, we extracted the aperiodic component over the 2-55 Hz frequency range of each power spectrum (*aperiodic_mode* = 'fixed', *peak_width_limits* = [2.66 (or 2 times the frequency resolution of each power spectrum), 12], *peak_threshold* = 3, and default settings otherwise). The negative of the corresponding aperiodic exponent was used to index aperiodic slope (Voytek et al., 2015; Gao et al., 2017).

High-Frequency Activity (HFA)

To generate HFA time series, data was bandpass filtered from 80-150 Hz using a one-way, Hamming-windowed sinc FIR filter with filter order corresponding to a 100-ms time window. HFA time series were then separately averaged within the pre- and late-encoding time windows by calculating the mean HFA value within each window.

Theta Identification

Data was lowpass filtered below 200 Hz using a one-way, Hamming-windowed sinc FIR filter using default filter order and transition width settings from the FieldTrip software toolbox. Data was then epoched into trials from -750 to 1600 ms relative to word presentation. Each trial was tapered with a Hanning window, and a power spectrum per trial was constructed using the absolute value squared of the complex-numbered output of the Discrete Fourier Transform. The median power spectrum across trials per electrode was calculated, and this average power spectrum was then decomposed using the FOOOF algorithm in order to detect oscillatory peaks in the 4-8 Hz oscillatory theta range (*aperiodic_mode* = 'fixed', *peak_width_limits* = [1, 12], *peak_threshold* = 1, and default settings otherwise). In this manner, theta center frequency was determined individually per channel. In the event that more than one peak was detected in the 4-8 Hz frequency range for an electrode, FOOOF-extracted bandwidths were used to determine the upper and lower frequency edges of each peak, and the average of the lowest frequency edge and the highest frequency edge across theta peaks was used as the theta center frequency. An electrode was considered as having prominent theta oscillations if at least one theta-frequency peak was detected.

Theta-HFA Phase-Amplitude Coupling (PAC)

Individual theta center frequency per patient was calculated as the mean theta center frequency across electrodes. To generate theta phase time series, data was bandpass filtered using a one-way, Hamming-windowed sinc FIR filter with a 4-Hz bandpass centered around individual theta center frequency and default filter order and transition width settings from the FieldTrip software toolbox. Theta phase time series

were extracted using the angle of the Hilbert transform of bandpass-filtered data. Phase time series and HFA time series were used to calculate PAC during the pre- and late-encoding time windows as described in Ozkurt and Schnitzler (2011).

Statistical Analysis

Subsequently Recalled vs. Non-Recalled Words

In comparing neural activity features between subsequently recalled versus non-recalled trials, only data from the first 15 lists with at least two remaining trials each were analyzed. This restriction was done to approximately standardize trial number across patients and to mitigate any practice effects or inter-session variability in performance or neural activity. The median trial number for the first 15 lists with at least two remaining trials each was 154.5 (minimum 80, maximum 178). Neural activity features were calculated per time window, trial, and channel. Subsequently, two-sample t-tests comparing neural activity features between subsequently recalled versus non-recalled words were used to generating corresponding t-statistics for each channel. T-statistics were then averaged separately across LTL and LFC electrodes by taking the mean value per region, and t-statistics were subjected to two-sided Wilcoxon signed rank tests to test across-patient significance.

Number of Items in Memory

As above, only data from the first 15 lists with at least two clean trials each were analyzed. Separately for pre- and late-encoding time windows, the difference in neural activity features between the first and last available clean trials per list were calculated

for each list and electrode. Recall per list was calculated as the percentage of words successfully recalled across only clean trials within each list. Per electrode, Spearman's correlation across lists was used to test the relationship between list recall and the changes in neural activity features from the beginning to end of lists. Spearman's *r* values were then averaged separately across LTL and LFC channels by taking the mean value per region, and Spearman's *r* values were subjected to two-sided Wilcoxon signed rank tests to test across-patient significance.

Classifier Performance

To test whether certain neural activity features could be used to successfully predict successful memory encoding and subsequent recall, L_2-regularized logistic regression models were constructed separately per patient using the *LogisticRegressionCV* function from the *sklearn.linear_model* Python module. For this approach and due to generally low trial numbers, particularly for subsequently recalled words, neural activity features from all available trials were used in order to potentially improve training and classifier performance. For each patient, neural activity features from all trials were split into 70% and 30% training and test partitions. The percentage of subsequently recalled versus non-recalled trials was balanced between training and test partitions, and training and test partitions were scaled to have zero mean and unit variance based on neural activity features from the training partition. An L_2-regularized logistic regression model was then trained using stratified five-fold cross-validation on the training partition. For this training, balanced class weights and area under the receiver operator curve (ROC) were used for scoring, and 10 regularization values (1/*C*,

with C ranging logarithmically between 10^{-4} and 10^{4}) were tested. The model was then re-trained using the full training partition and the regularization value corresponding to highest classifier performance, after which the performance of the fully trained model was assessed using the test partition. This procedure was repeated using 1000 random training and test partitions per patient, and median classifier performance across the random partitions was calculated. Classifier performance was compared between groups of models trained using different neural activity features using two-sided Wilcoxon signed rank tests.

Results

Behavior

We analyzed previously collected behavioral data from 105 patients with electrocorticographic (ECoG) or stereotactic encephalographic (sEEG) implants performing a delayed verbal recall task (Burke et al., 2013; Solomon et al., 2017; Ezzyat et al., 2018). In this task, lists of serially presented words were visually presented to patients, and after each list, patients were asked to recall as many words as possible from the immediately previous list (Figure 3.1A). Across these patients, recall percentage declined with increasing age (Figure 3.1B, Spearman's $r = -0.34$, $p < 10^{-3}$).

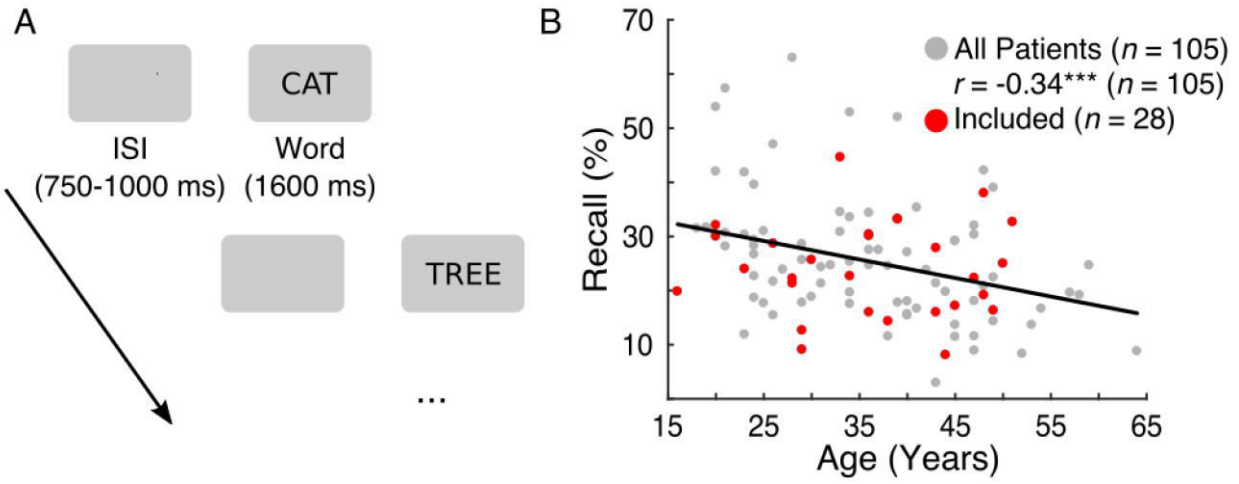

Figure 3.1. Delayed free recall task and behavioral performance. (A) Patients performed a delayed free recall task in which lists of 12 visually, serially presented words were provided. At the end of each list, patients performed a 20-second distractor task before having 30 seconds to verbalize in any order any words from the previous list (not shown here). (B) Percent recall performance by age for 105 patients (shown in gray). Recall performance declined with increasing age (*** $p < 0.001$). Twenty-eight patients (shown in red) were included in subsequent electrophysiological analyses.

Electrophysiological Markers

Of these patients, 28 patients (17 female, 11 male) with surface (*i.e.*, ECoG) electrodes implanted over both the lateral temporal lobe (LTL) and the lateral frontal cortex (LFC) were selected for further analysis. For these patients, recall percentage was uncorrelated with age ($p = 0.96$).

We sought to determine if characteristics of aperiodic activity differed either before or during the presentation of subsequently recalled versus non-recalled words. To do so, we examined 1/*f*-like aperiodic slope and high-frequency activity (HFA) in both the LTL and the LFC. Both aperiodic slope and HFA were calculated for pre-encoding (-750-0 ms relative to word presentation) and late-encoding (800-1600 ms relative to word presentation) time windows.

We also examined LTL and LFC theta-HFA phase-amplitude coupling (PAC). In order to so, we identified electrodes in which a prominent peak in the 4-8 Hz frequency range of the electrophysiological power spectrum was observed (*i.e.,* a peak with power sufficiently above that of surrounding frequencies). Theta oscillations were more prominent in LFC over LTL electrodes (median 100% vs. 83%, $W = 38$, $p = 0.0054$).

Subsequently Recalled vs. Non-Recalled Words

We compared pre- and late-encoding LTL and LFC aperiodic slope between subsequently recalled versus non-recalled words. Pre-encoding LFC aperiodic slope was higher (flatter) for subsequently recalled versus non-recalled words (Figure 3.2A, median aperiodic slope -1.77 vs. -1.80, median *t*-statistic 0.18, $W = 299$, $p = 0.029$). There was no such difference for late-encoding LFC aperiodic slope ($p = 0.19$), pre-

encoding LTL aperiodic slope (p = 0.28), or late-encoding LTL aperiodic slope (p = 0.40).

We also compared pre- and late-encoding LTL and LFC HFA between subsequently recalled versus non-recalled words. Late-encoding LFC HFA was higher for subsequently recalled versus non-recalled words (Figure 3.2B, median HFA 2.52 vs. 2.45, median t-statistic 0.44, W = 319, p = 0.0071). There was no such difference for pre-encoding LFC HFA (p = 0.32), pre-encoding LTL HFA (p = 0.34), or late-encoding LTL HFA (p = 0.75).

Finally, we compared pre- and late-encoding LTL and LFC theta-HFA PAC between subsequently recalled versus non-recalled words. When considering all electrodes, there was no difference in theta-HFA PAC during either pre-encoding (LTL: p = 0.47, LFC: p = 0.92) or late-encoding (LTL: p = 0.27, LFC: p = 0.40) time windows. When considering only electrodes displaying prominent theta oscillations, only 26 patients had at least three such electrodes in each of the LTL and the LFC. For these patients, there was no difference in theta-HFA PAC during either pre-encoding (LTL: p = 0.44, LFC: p = 0.88) or late-encoding (LTL: p = 0.88, LFC: p = 0.52) time windows when analyzing only electrodes with prominent theta oscillations (Figure 3.2C).

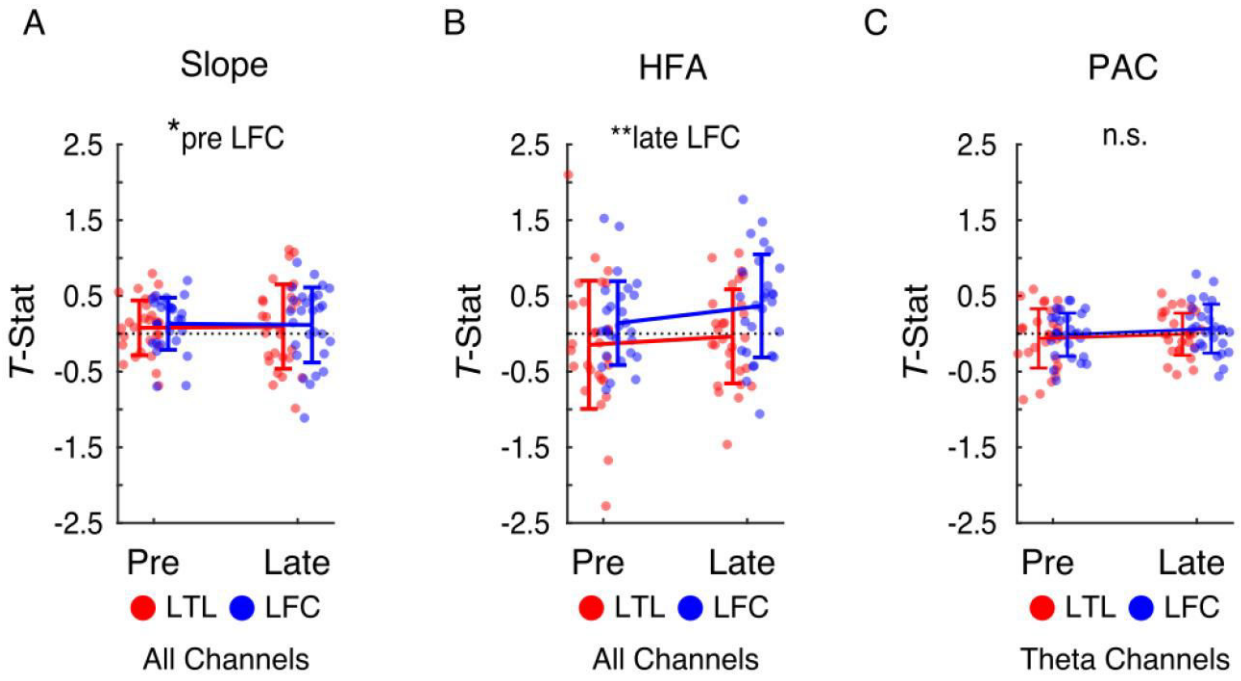

Figure 3.2. Comparison of pre- (-750-0 ms) and late-encoding (800-1600 ms) lateral temporal lobe (LTL, shown in red) and lateral frontal cortical (LFC, shown in blue) neural activity between subsequently recalled versus non-recalled words. (A) Pre-encoding LFC 1/*f*-like aperiodic slope was higher (flatter) for subsequently recalled versus non-recalled words (*$p < 0.05$, bars of mean ± standard deviation). (B) Late-encoding LFC 80-150 Hz high-frequency activity (HFA) was higher for subsequently recalled versus non-recalled words (**$p < 0.01$, bars of mean ± standard deviation). (C) No differences were observed between subsequently recalled versus non-recalled words for 4-8 Hz theta-HFA phase-amplitude coupling (PAC, bars of mean ± standard deviation).

Number of Items in Memory

We also sought to determine if changes in aperiodic activity from the beginning to the end of each list might track the number of words subsequently recalled on that list. To do so, we calculated separately per time window and electrode the differences in aperiodic slope and HFA between the first and last available words per list, and we correlated per electrode these difference values with percent recall on individual lists (see Figure 3.3A for an example electrode). Averaging within regions, we found that while pre-encoding LFC aperiodic slope on average decreased between the first and the last word of each list (median difference -0.054, $W = 115$, $p = 0.045$), it increased during lists with higher percent recall (Figure 3.3B, median Spearman's $r = 0.046$, $W = 301$, $p = 0.025$). No such changes were found for pre-encoding LTL aperiodic slope ($p = 0.80$), late-encoding LTL aperiodic slope ($p = 0.76$), or late-encoding LFC aperiodic slope ($p = 0.16$), nor were such changes found for HFA during either pre-encoding (LTL: $p = 0.96$; LFC: $p = 0.45$) or late-encoding (LTL: $p = 0.75$; LFC: $p = 0.42$) time windows (Figure 3.3C).

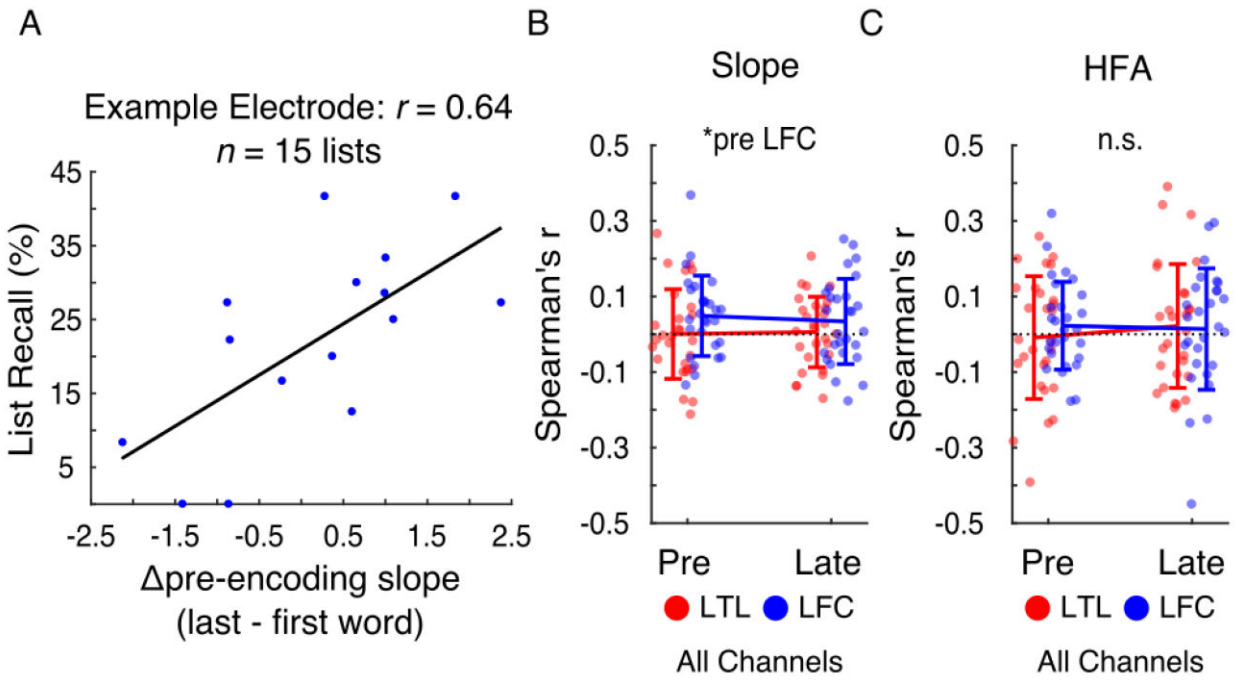

Figure 3.3. Relationship between LTL and LFC aperiodic slope and HFA and the number of memory items maintained. (A) For this example electrode, pre-encoding LFC aperiodic slope increased (became flatter) between the first and last word of lists in which more words were subsequently recalled. (B) Across patients, pre-encoding LFC aperiodic slope increased from the beginning to end of lists with higher percent recall (*$p < 0.05$, bars of mean ± standard deviation). (C) No such relationship was observed for HFA (bars of mean ± standard deviation).

Predicting Encoding

Finally, we determined if pre-encoding LFC aperiodic slope or late-encoding LFC HFA could be used to predict successful memory encoding. To do so, we constructed individualized L_2-regularized logistic regression models trained to classify aperiodic slope and HFA between subsequently recalled versus non-recalled words. Across patients, models trained using pre-encoding LFC aperiodic slope had median classifier performance of 0.50 (*i.e.,* at chance), as measured using the area under the receiver operating curve (AUC). Models trained using late-encoding LFC HFA had median classifier performance of 0.56. Classifier performance was higher for models trained using late-encoding LFC HFA than with pre-encoding LFC aperiodic slope (median AUC 0.56 vs. 0.50, $W = 316$, $p = 0.0089$).

Discussion

In this study, we investigated differences in aperiodic activity that distinguish successful from unsuccessful memory encoding. We found that successful memory encoding was associated with higher pre-stimulus LFC aperiodic slope and post-stimulus LFC HFA. We also found that pre-stimulus LFC aperiodic slope increased as more and more memory items were successfully encoded. Theta-HFA PAC did not differ between episodes of successful versus unsuccessful memory encoding in either the LTL or LFC.

Our finding that post-stimulus LFC HFA was higher during successful versus unsuccessful memory encoding recapitulates similar findings (Burke et al., 2013; Solomon et al., 2017; Ezzyat et al., 2018) and provides further evidence for the role of

asynchronous population spiking in memory encoding (Manning et al., 2009; Miller et al., 2012). Interestingly, we did not find any differences in post-stimulus aperiodic slope between successful versus unsuccessful memory encoding. This lack of difference suggests that previous findings showing power reductions in low-frequency activity during successful memory encoding (Burke et al., 2013) are driven primarily by changes in theta oscillatory activity. That post-stimulus LFC aperiodic slope and HFA were not both associated with successful memory encoding suggests that different information about underlying neural activity can be gained from examining either measure. Specifically, this suggests distinct underlying neural sources with potentially dissociable roles in memory formation.

Previous findings have shown that more desynchronized brain states facilitate the processing and encoding of sensory information (Marguet and Harris, 2011; Pachitariu et al., 2015). In that reductions in low-frequency power relative to high-frequency power might similarly reflect desynchronized brain states, our finding that pre-stimulus LFC aperiodic slope was higher (flatter) prior to the presentation of subsequently recalled versus non-recalled words suggests that desynchronized LFC brain states might also improve the likelihood of successful memory encoding, subsequent recall, or both. That being said, post-stimulus LFC HFA was a much stronger indicator of successful memory encoding than was pre-stimulus LFC aperiodic slope, suggesting that LFC brain state might only weakly impact subsequent memory encoding and recall. Our findings also suggest that LFC brain states become more desynchronized as more items are maintained in short-term memory.

Limitations of the present study include that relatively expansive brain regions (LTL and LFC) and time periods (-750-0 ms and 800-1600 ms relative to memory item presentation) were examined. Presently observed memory-related differences in LFC aperiodic slope and HFA suggest the widespread prevalence of such effects across multiple subregions of the LFC. At the same time, specific examination of smaller subregions or shorter time windows will be necessary to further elucidate neural mechanisms contributing to memory encoding, especially regarding the LTL and perhaps theta-HFA PAC.

Chapter 3, in full, is currently being prepared for submission for publication of the material. Tran, T. T. & Voytek B. Frontal cortical aperiodic activity tracks successful memory encoding. The dissertation author was the primary investigator and author of this paper.

References

Axmacher, N., Henseler, M.M., Jensen, O., Weinreich, I., Elger, C.E., Fell, J., 2010. Cross-frequency coupling supports multi-item working memory in the human hippocampus. Proc. Natl. Acad. Sci. U.S.A. 107, 3228–3233.

Burke, J.F., Zaghloul, K.A., Jacobs, J., Williams, R.B., Sperling, M.R., Sharan, A.D., Kahana, M.J., 2013. Synchronous and asynchronous theta and gamma activity during episodic memory formation. J. Neurosci. 33, 292–304.

Canolty, R.T., Edwards, E., Dalal, S.S., Soltani, M., Nagarajan, S.S., Kirsch, H.E., Berger, M.S., Barbaro, N.M., Knight, R.T., 2006. High gamma power is phase-locked to theta oscillations in human neocortex. Science 313, 1626–1628.

Ezzyat, Y., Wanda, P.A., Levy, D.F., Kadel, A., Aka, A., Pedisich, I., Sperling, M.R., Sharan, A.D., Lega, B.C., Burks, A., Gross, R.E., Inman, C.S., Jobst, B.C., Gorenstein, M.A., Davis, K.A., Worrell, G.A., Kucewicz, M.T., Stein, J.M., Gorniak, R., Das, S.R., Rizzuto, D.S., Kahana, M.J., 2018. Closed-loop stimulation of temporal cortex rescues functional networks and improves memory. Nat Comms 9, 365–8.

Fries, P., 2005. A mechanism for cognitive dynamics: neuronal communication through neuronal coherence. Trends in Cognitive Sciences 9, 474–480.

Gao, R., Peterson, E.J., Voytek, B., 2017. Inferring synaptic excitation/inhibition balance from field potentials. NeuroImage 158, 70–78.

Haller, M., Donoghue, T., Peterson, E., Varma, P., Sebastian, P., Gao, R., Noto, T., Knight, R.T., Shestyuk, A., Voytek, B., 2018. Parameterizing neural power spectra. bioRxiv 299859.

Lega, B., Burke, J., Jacobs, J., Kahana, M.J., 2015. Slow-Theta-to-Gamma Phase–Amplitude Coupling in Human Hippocampus Supports the Formation of New Episodic Memories. Cerebral Cortex 26, 268–278.

Manning, J.R., Jacobs, J., Fried, I., Kahana, M.J., 2009. Broadband shifts in local field potential power spectra are correlated with single-neuron spiking in humans. J. Neurosci. 29, 13613–13620.

Marguet, S.L., Harris, K.D., 2011. State-dependent representation of amplitude-modulated noise stimuli in rat auditory cortex. J. Neurosci. 31, 6414–6420.

Maris, E., van Vugt, M., Kahana, M., 2011. Spatially distributed patterns of oscillatory coupling between high-frequency amplitudes and low-frequency phases in human iEEG. NeuroImage 54, 836–850.

Miller, K.J., Sorensen, L.B., Ojemann, J.G., Nijs, den, M., 2009. Power-Law Scaling in the Brain Surface Electric Potential. PLoS Comput Biol 5, e1000609.

Oostenveld, R., Fries, P., Maris, E., Schoffelen, J.-M., 2011. FieldTrip: Open Source Software for Advanced Analysis of MEG, EEG, and Invasive Electrophysiological Data. Computational Intelligence and Neuroscience 2011, 1–9.

Özkurt, T.E., Schnitzler, A., 2011. A critical note on the definition of phase-amplitude cross-frequency coupling. Journal of Neuroscience Methods 201, 438–443.

Pachitariu, M., Lyamzin, D.R., Sahani, M., Lesica, N.A., 2015. State-dependent population coding in primary auditory cortex. J. Neurosci. 35, 2058–2073.

Parvizi, J., Kastner, S., 2018. Promises and limitations of human intracranial electroencephalography. Nature Neuroscience 21, 474–483.

Podvalny, E., Noy, N., Harel, M., Bickel, S., Chechik, G., Schroeder, C.E., Mehta, A.D., Tsodyks, M., Malach, R., 2015. A unifying principle underlying the extracellular field potential spectral responses in the human cortex. Journal of Neurophysiology 114, 505–519.

Solomon, E.A., Kragel, J.E., Sperling, M.R., Sharan, A., Worrell, G., Kucewicz, M., Inman, C.S., Lega, B., Davis, K.A., Stein, J.M., Jobst, B.C., Zaghloul, K.A., Sheth, S.A., Rizzuto, D.S., Kahana, M.J., 2017. Widespread theta synchrony and high-frequency desynchronization underlies enhanced cognition. Nat Comms 8, 1704–14.

Tort, A.B.L., Komorowski, R.W., Manns, J.R., Kopell, N.J., Eichenbaum, H., 2009. Theta-gamma coupling increases during the learning of item-context associations. Proc. Natl. Acad. Sci. U.S.A. 106, 20942–20947.

van der Meij, R., Kahana, M., Maris, E., 2012. Phase-Amplitude Coupling in Human Electrocorticography Is Spatially Distributed and Phase Diverse. Journal of Neuroscience 32, 111–123.

Voytek, B., Canolty, R.T., Shestyuk, A., Crone, N.E., Parvizi, J., Knight, R.T., 2010. Shifts in gamma phase-amplitude coupling frequency from theta to alpha over posterior cortex during visual tasks. Front. Hum. Neurosci. 4, 191.

Voytek, B., Kramer, M.A., Case, J., Lepage, K.Q., Tempesta, Z.R., Knight, R.T., Gazzaley, A., 2015. Age-Related Changes in 1/f Neural Electrophysiological Noise. J. Neurosci. 35, 13257–13265.

CONCLUSION

In this dissertation, I document findings from three studies. In Chapter 1, I show using EEG that higher trial-by-trial variability in the visual cortical alpha phase response to task-relevant stimuli is associated both with healthy aging and with reduced behavioral performance in a visual short-term memory task. In Chapter 2, I show that in healthy aging, higher trial-by-trial variability in the alpha phase response is associated with the age-related flattening of visual cortical baseline 1/*f* slope. In Chapter 3, I show using ECoG recordings that trial-by-trial shifts in pre-stimulus frontal cortical 1/*f* slope can help distinguish between episodes of successful versus unsuccessful memory encoding. I also show that the flattening of frontal cortical 1/*f* slope indexes the number of items maintained and subsequently recalled from memory.

These findings could be expanded on in future work. For instance, regarding Chapter 2, older adults had higher variability in their alpha phase response to visual targets. However, unlike younger adults, the degree of alpha phase response variability was not correlated with overall behavioral performance. This difference between younger and older adults may be due to compensatory mechanisms in older adults, changes in visual stimulus processing that account for or counteract higher stimulus-evoked response variability. However, in Chapter 2, trials from both spatially cued and non-cued trials were pooled together, during the latter of which older adults had lower performance than younger adults. Additional experiments, perhaps with just one cued condition and one uncued condition, would allow for deeper examination of any age-related differences in pre-target or target-evoked activity separately for cued and non-cued trials, especially in any neural markers subsequent to initial target-evoked alpha

phase responses. These additional experiments would help resolve any age-related differences in neural activity, behavior, or relationships between not reported in Chapter 2 as well as elucidate the nature of any age-related compensatory mechanisms.

Regarding Chapter 3, additional analyses could be used to determine smaller time windows and subregions within the lateral temporal lobe and the lateral frontal cortex that display memory encoding-related changes in high-frequency activity or 1/*f* slope. Similar analyses as used in Chapter 3 could also be conducted on sEEG recordings, which would allow for the examination of more brain regions as well as the comparison of memory-related effects between ECoG and sEEG recordings.

In addition, failures in recall can be attributable to failures either in initial memory encoding or in retrieval after successful memory encoding. As a result, a confound of the results presented in Chapter 3 is that neural activity during the presentation of non-recalled words may reflect either successful or unsuccessful memory encoding. Additional analyses could help truly separate episodes of successful versus unsuccessful memory encoding during trials for which words were not subsequently recalled. A possible approach would be to use clustering techniques on extracted neural activity features in order to find two distinct groups of trials, these groups corresponding to successful and unsuccessful memory encoding. It is also possible that more than two distinct groups will be discovered, these additional groups likely reflecting other types of failures that would affect subsequent recall.

It is my hope that this work helps further our understanding of the neural processes supporting attention and memory and how some of these processes may be altered during healthy aging. It has been a privilege to have been able to take this time

and opportunity to explore brain function, its impact on behavior, and what it is we can learn from human electrophysiological recordings. I am grateful for all of it, and I know that because of this training, I am prepared for any future challenges and opportunities coming my way.